

# On the effect of hyperaldosteronism-inducing mutations in Na/K pumps

Dylan J. Meyer,<sup>1,2</sup> Craig Gatto,<sup>2</sup> and Pablo Artigas<sup>1</sup>

<sup>1</sup>Department of Cell Physiology and Molecular Biophysics, Center for Membrane Protein Research, Texas Tech University Health Sciences Center, Lubbock, TX

<sup>2</sup>School of Biological Sciences, Illinois State University, Normal, IL

Primary aldosteronism, a condition in which too much aldosterone is produced and that leads to hypertension, is often initiated by an aldosterone-producing adenoma within the zona glomerulosa of the adrenal cortex. Somatic mutations of ATP1A1, encoding the Na/K pump  $\alpha 1$  subunit, have been found in these adenomas. It has been proposed that a passive inward current transported by several of these mutant pumps is a "gain-of-function" activity that produces membrane depolarization and concomitant increases in aldosterone production. Here, we investigate whether the inward current through mutant Na/K pumps is large enough to induce depolarization of the cells that harbor them. We first investigate inward currents induced by these mutations in *Xenopus* Na/K pumps expressed in *Xenopus* oocytes and find that these inward currents are similar in amplitude to wild-type outward Na/K pump currents. Subsequently, we perform a detailed functional evaluation of the human Na/K pump mutants L104R, delF100-L104, V332G, and EETA963S expressed in *Xenopus* oocytes. By combining two-electrode voltage clamp with [<sup>3</sup>H]ouabain binding, we measure the turnover rate of these inward currents and compare it to the turnover rate for outward current through wild-type pumps. We find that the turnover rate of the inward current through two of these mutants (EETA963S and L104R) is too small to induce significant cell depolarization. Electrophysiological characterization of another hyperaldosteronism-inducing mutation, G99R, reveals the absence of inward currents under many different conditions, including in the presence of the regulator FXYP1 as well as with mammalian ionic concentrations and body temperatures. Instead, we observe robust outward currents, but with significantly reduced affinities for intracellular Na<sup>+</sup> and extracellular K<sup>+</sup>. Collectively, our results point to loss-of-function as the common mechanism for the hyperaldosteronism induced by these Na/K pump mutants.

## INTRODUCTION

Primary aldosteronism, a form of hyperaldosteronism, is the most common cause of secondary hypertension (Mulatero et al., 2004; Rossi et al., 2006; Hannemann et al., 2012). Normal aldosterone production by the adrenal cortex is regulated by Ca<sup>2+</sup> entry caused by membrane depolarization caused by angiotensin II or hyperkalemia (Spät, 2004). In primary aldosteronism, however, constitutive aldosterone production is observed in the absence of these physiological triggers. Approximately 50% of primary aldosteronism cases are caused by a unilateral aldosterone-producing adenoma within the zona glomerulosa of the adrenal cortex. Many of these adenomas harbor recurrent somatic mutations to genes encoding inward-rectifier K<sup>+</sup> channels (KCNJ5; Choi et al., 2011), L-type Ca<sup>2+</sup> channels (CACNA1D; Azizan et al., 2013), plasma membrane Ca<sup>2+</sup>-ATPase isoform 3 (ATP2B3; Beuschlein et al., 2013; Williams et al., 2014), and the  $\alpha 1$  subunit of the Na<sup>+</sup>,K<sup>+</sup>-ATPase (ATP1A1; Azizan et al., 2013; Beuschlein et al., 2013; Williams et al., 2014; Åkerström et al., 2015; Zheng et al., 2015). This paper focuses on Na<sup>+</sup>,K<sup>+</sup>-ATPase mutations.

The Na<sup>+</sup>,K<sup>+</sup>-ATPase (or Na/K pump) belongs to the class IIC of P-type ATPases. It utilizes the energy of ATP

hydrolysis to export 3 Na<sup>+</sup> in exchange for the import of 2 K<sup>+</sup> to build the electrochemical gradients for these ions across the plasma membrane. Normal ion gradients are essential for cellular excitability, secondary-active transport, and establishing the cell's resting membrane potential (important for regulating aldosterone production in adrenal zona glomerulosa cells). The minimal Na/K pump functional unit requires association of one catalytic  $\alpha$ -subunit ( $\alpha 1$ – $\alpha 4$ ) with one  $\beta$ -subunit ( $\beta 1$ – $\beta 3$ ; Blanco and Mercer, 1998). A regulatory FXYP subunit (FXYP1–FXYP7) is sometimes associated with the  $\alpha\beta$  dimer in a tissue-dependent manner (Geering, 2008). The  $\alpha$ -subunit has ten transmembrane (TM) segments housing the three ion-binding sites, and contains machinery for ATP binding and hydrolysis in its intracellular loops (Kaplan, 2002). The  $\beta$ -subunit has a single transmembrane segment and is required for enzyme stability and plasma membrane targeting (Gatto et al., 2001; Kaplan, 2002). All Na/K pump mutations in aldosterone-producing adenomas have been found within the transmembrane segments of the  $\alpha 1$  subunit, near ion-binding sites II and III (Fig. 1).

Correspondence to Pablo Artigas: pablo.artigas@ttuhsc.edu

Abbreviations used: MS, methanesulfonic acid; TEVC, two-electrode voltage clamp; TM, transmembrane.

© 2017 Meyer et al. This article is distributed under the terms of an Attribution–Noncommercial–Share Alike–No Mirror Sites license for the first six months after the publication date (see <http://www.rupress.org/terms/>). After six months it is available under a Creative Commons License (Attribution–Noncommercial–Share Alike 4.0 International license, as described at <https://creativecommons.org/licenses/by-nc-sa/4.0/>).



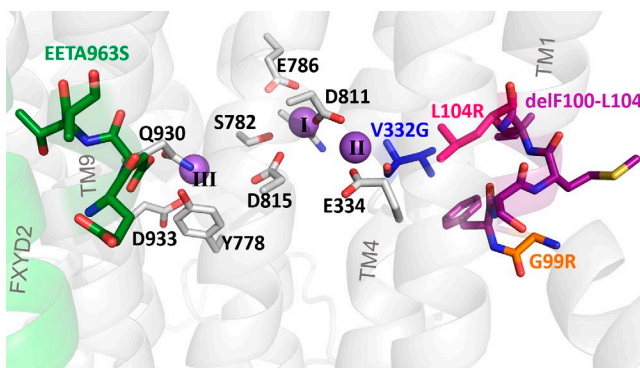


**Figure 1. Location of hyperaldosteronism mutations.** Zoomed-in view of the ion-binding sites in the E1(3Na) pig Na/K pump structure (Protein Data Bank accession no. 2ZXE) indicating several ion-coordinating residues. The three Na<sup>+</sup> ions bound are shown in purple, and the carbon backbone of residues altered by hyperaldosteronism-associated Na/K pump mutations studied here is the same color scheme used for each mutant throughout the article.

Fig. 1 shows an enlarged view of the Na<sup>+</sup>-bound pig kidney ( $\alpha 1\beta 1$ FXD2) Na/K pump structure (Kanai et al., 2013) highlighting the location of the five mutations studied in this article. These mutations include the single substitutions G99R (orange carbons) and L104R (pink carbons), both in TM1; the deletion of five residues (delF100-L104, purple carbons), also in TM1; the single substitution V332G (blue carbons) in TM4; and the substitution EETA963S (green carbons) in TM9, where two glutamates, a threonine, and an alanine are replaced by a single serine at position 963.

In the first article describing the association between mutations L104R, V332G, and delF100-L104 and primary aldosteronism, Beuschlein et al. (2013) reported that cells from aldosterone-producing adenomas presented a ~20-mV depolarization of the resting membrane potential. This observation, together with the recurrence of a few mutations, led to the proposal of a "gain-of-function" in these mutant pumps. Azizan et al. (2013) discovered the EETA963S mutation and found that when expressed in *Xenopus* oocytes, L104R, V332G, delF100-L104, and EETA963S all carry an inward current in the presence of near-physiological Na<sup>+</sup><sub>o</sub>, a finding consistent with a depolarizing gain-of-function. More recently, variants of the deletion mutants, as well as G99R, were discovered (Williams et al., 2014; Åkerström et al., 2015; Zheng et al., 2015). Although G99R has not been evaluated electrophysiologically in detail, it is believed to behave similarly to other TM1 and TM4 mutations (Williams et al., 2014; Åkerström et al., 2015; Gomez-Sanchez et al., 2015; Azizan and Brown, 2016).

Under conditions where hyperaldosteronism mutants generate inward current (i.e., at physiological [Na<sup>+</sup><sub>o</sub>] and [K<sup>+</sup><sub>o</sub>]), wild-type Na/K pumps generate

outward current caused by the unbalanced transport of 3 Na<sup>+</sup> for 2 K<sup>+</sup>. It is well known that in most cells, this hyperpolarizing current contributes little to the resting voltage (Sachse et al., 2017). However, at subsaturating Na<sup>+</sup><sub>o</sub> and K<sup>+</sup><sub>o</sub>, when in the extracellularly facing E2P conformation (Stanley et al., 2016), wild-type pumps exhibit a passive inward H<sup>+</sup> current at negative voltages (Wang and Horisberger, 1995). It is thought that these protons transit the Na<sup>+</sup>-exclusive binding site (site III), as shown by extensive mutagenesis of residues critical for Na<sup>+</sup> binding at site III (Vedovato and Gadsby, 2014) and characterization of the voltage dependence of H<sup>+</sup> transport affinity (Mitchell et al., 2014). The proposed gain-of-function inward currents observed in hyperaldosteronism-associated TM1 and TM4 mutants were suggested to transit a pathway separate from the inward current through either wild type or the TM9 mutant EETA963S (Kopeck et al., 2014).

In this article, we present a study originally designed to examine the ion pathways of inward currents through hyperaldosteronism Na/K pump mutants. We observed that the inward currents through these mutants were of relatively small magnitude. Given that only half the Na/K pump population is mutated in aldosterone-producing adenoma cells (i.e., a monoallelic mutation; Beuschlein et al., 2013), and because the resting membrane potential is set by TASK K<sup>+</sup> channels within the adrenal zona glomerulosa (Spät, 2004), one would expect that a current capable of inducing a ~20-mV depolarization would be of significantly larger magnitude than the wild-type pump outward current. Therefore, we performed a detailed evaluation of the inward current through L104R, V332G, delF100-L104, or EETA963S. Using a combination of two-electrode voltage clamp (TEVC) and [<sup>3</sup>H]ouabain binding, we obtained the turnover rates of the inward "leak" currents through each hyperaldosteronism-associated human  $\alpha 1$  mutant and the wild-type outward pump currents. Our data show that inward currents through two mutants have amplitudes that are smaller than or comparable with outward wild-type pump currents.

These findings also prompted us to characterize the function of G99R using TEVC and inside-out patch clamp. To our surprise, G99R lacked inward currents in the presence of Na<sup>+</sup><sub>o</sub> and K<sup>+</sup><sub>o</sub>, instead presenting outward currents with significantly reduced affinities for K<sup>+</sup><sub>o</sub> and Na<sup>+</sup><sub>i</sub>. Collectively, our results demonstrate that inward current cannot be the common gain-of-function mechanism underlying the generation of primary aldosteronism. Thus, a loss-of-function seems to be the primary mechanism by which Na/K pump  $\alpha 1$  mutants contribute to constitutive aldosterone production in aldosterone-producing adenomas, which then leads to development of hyperaldosteronism, hypokalemia, and hypertension.

## MATERIALS AND METHODS

### Oocyte isolation, molecular biology, and Western blotting

Oocytes were isolated, enzymatically defolliculated, and cultured as previously described (Stanley et al., 2015, 2016). All mutations were introduced by site-directed mutagenesis and confirmed by DNA sequencing. Plasmid DNA, in the pSD5 vector, was linearized using NdeI (for human  $\alpha 1$ ) or BglIII (for human  $\beta 1$ , *Xenopus*  $\alpha 1$ , and *Xenopus*  $\beta 3$ ). The SP6 mMessage machine kit (Ambion) was used for cRNA in vitro transcription. Healthy oocytes were injected with equimolar cRNA mixtures of human  $\alpha 1$  with human  $\beta 1$  or a *Xenopus* ouabain-resistant template Q120R/N131D (RD)- $\alpha 1$  with *Xenopus*  $\beta 3$  (50 ng  $\alpha$ , 17 ng  $\beta$ ) and kept at 16°C until recording in SOS solution ([mM] 100 NaCl, 2 KCl, 1.8 CaCl<sub>2</sub>, 1 MgCl<sub>2</sub>, and 5 HEPES) supplemented with horse serum and antimycotic-antibiotic solution (Gibco Anti-Anti; Thermo Fisher Scientific). For simplicity, human numbering is used throughout (*Xenopus*  $\alpha 1$  numbering is two positions higher than human  $\alpha 1$ ). In one set of experiments (Fig. 9 B), human  $\alpha 1\beta 1$  cRNA was coinjected with equimolar human FXD1 cRNA.

The RD mutations that make the rat  $\alpha 1$  Na/K pump resistant to ouabain (IC<sub>50</sub> ~100  $\mu$ M, Price and Lingrel, 1988) are commonly introduced to separate the electrical signals of exogenous and endogenous pumps (Koenderink et al., 2003; Azizan et al., 2013; Stanley et al., 2016). These mutations were present in our *Xenopus* pumps (throughout the Results section, the letters RD precede the name of all *Xenopus* mutants). However, most hyperaldosteronism mutations further reduce ouabain affinity (compare Fig. 2, Fig. 3, and Fig. S1). Therefore, we chose not to introduce RD mutations into the human pumps to avoid unintended functional consequences (Vedovato and Gadsby, 2010) and to allow for [<sup>3</sup>H]ouabain measurements. We consistently achieved exogenous expression levels 15–20-fold greater than endogenous pump levels 4 d after injection, as we have previously reported using human pumps (Stanley et al., 2015).

**Western blotting.** 20–25 oocytes were suspended in 7.5 ml buffer HS ([mM] 25 imidazole, 1 EDTA, and 250 sucrose, pH 7.4) and homogenized with six strokes in a 15-ml Wheaton homogenizer. Cellular debris was pelleted via centrifugation at 400 g (20 min at 4°C) and discarded. The supernatant was layered on top of 30 ml of 20% sucrose solution (prepared in 25 mM imidazole and 1 mM EDTA, pH 7.4) and spun through the sucrose at 112,700 g. The resulting pellet contained the enriched plasma membrane fraction, which was used for Western blot analyses. 0.5  $\mu$ g of purified sheep kidney Na<sup>+</sup>,K<sup>+</sup>-ATPase and 20  $\mu$ g of enriched plasma membrane from *Xenopus* oocytes were solubilized with 25  $\mu$ l

of 4× Laemmli sample buffer (1:1:1 [vol/vol/vol] of 8 M urea, 10% SDS, and 125 mM Tris-HCl, pH 6.8, and 5%  $\beta$ -mercaptoethanol), and proteins were resolved on a 7.5% SDS-PAGE gel according to the method of Laemmli (Laemmli, 1970). After electrophoresis, proteins were transferred onto PVDF membranes by electroblotting in 10 mM CAPS and 10% MeOH, pH 11.0, for 2 h at 180-mA constant current (Matsudaira, 1987). The PVDF membrane was blocked with 10% soy milk solution in phosphate-buffered saline for 1 h (Galva et al., 2012). The membrane was then incubated with an antibody against the Na<sup>+</sup>,K<sup>+</sup>-ATPase C terminus (anti-KET Y; 1:1,000) for 1 h at room temperature. The primary antibody was removed, and the membrane was washed three times with phosphate-buffered saline plus 0.1% Tween 20 and then incubated for 1 h with HRP-conjugated secondary anti-rabbit IgG at room temperature (1:5,000). The membrane was then washed five times with phosphate-buffered saline plus 0.1% Tween 20, and the proteins were visualized by chemiluminescent detection of peroxidase activity using the SuperSignal West Pico substrate kit (Thermo Scientific).

### Electrophysiology

TEVC was performed with an OC-725C amplifier (Warner Instruments) or a CA-1B amplifier (Dagan). Data were acquired with a digidata A/D converter at 10 kHz and with a Minidigi 1A at slower rates, all controlled with pClamp 10 software (digidata, mindigi, and pClamp; Molecular Devices). Glass electrodes were backfilled with 3 M KCl (resistances of 0.2–1.0 M $\Omega$ ). Oocytes expressing human or *Xenopus* pumps were Na<sup>+</sup> loaded for 30 min (to saturate intracellular Na<sup>+</sup> binding) in a solution containing (mM) 90 NaOH, 20 tetraethylammonium (TEA)-OH, 0.2 EGTA, and 40 HEPES, pH 7.2, with sulfamic acid, supplemented with 10  $\mu$ M ouabain only in experiments with the RD- $\alpha 1\beta 3$  from *Xenopus*. The standard external solutions contained (mM) 133 methanesulfonic acid (MS), 5 Ba(OH)<sub>2</sub>, 1 Mg(OH)<sub>2</sub>, 0.5 Ca(OH)<sub>2</sub>, 10 HEPES, and 125 NMG (NMG<sup>+</sup> solution) or 125 NaOH (Na<sup>+</sup> solution), pH 7.6. External K<sup>+</sup> was added from a 450-mM K-MS stock. With the intention to mimic a more mammalian-like extracellular environment, some K<sup>+</sup> titration experiments were performed at higher Na<sup>+</sup> concentrations in external solutions made by mixing buffers containing (mM) 150 NaOH or 150 KOH, 5 BaCl<sub>2</sub>, 1 MgCl<sub>2</sub>, 0.5 CaCl<sub>2</sub>, and 5 HEPES, titrated to pH 7.4 with MS. Ouabain was directly dissolved in external solutions.

Giant inside-out patch clamp was performed with a Dagan 3900A amplifier acquired at 100 kHz with a digidata 1550A A/D board and at 1 kHz with a minidigi 1A and pClamp software. Borosilicate glass pipettes (WPI) were pulled and fire polished to a diameter of ~20  $\mu$ m and coated with Sylgard. Patches were formed exclusively on the animal pole of devitellinized oocytes in a



bath containing (mM) 100 KOH, 100 L-aspartic acid, 20 KCl, 10 HEPES, 4 MgCl<sub>2</sub>, and 2 EGTA, pH 7.0, with KOH. Pipettes were filled with a solution containing (mM) 140 NMg, 5 KCl, 5 BaCl<sub>2</sub>, 1 MgCl<sub>2</sub>, 0.5 mM CaCl<sub>2</sub>, and 5 HEPES, titrated to pH 7.4 with HCl. Excised patches were held at 0 mV and perfused with mixtures of intracellular solutions containing (mM) 1 MgCl<sub>2</sub>, 10 TEA-Cl, 5 EGTA, 5 HEPES, 20 L-glutamic acid, and 140 NaOH (Na<sup>+</sup><sub>i</sub> solution), 140 NMg<sup>+</sup> (NMg<sup>+</sup><sub>i</sub> solution), or 140 KOH (K<sup>+</sup><sub>i</sub> solution) titrated to pH 7.4 with L-glutamic acid. Intermediate Na<sup>+</sup><sub>i</sub> concentrations were obtained by mixing solutions (Na<sup>+</sup><sub>i</sub> with K<sup>+</sup><sub>i</sub> in Fig. 10 or Na<sup>+</sup><sub>i</sub> with NMg<sup>+</sup><sub>i</sub> in Fig. S3). Na/K pump currents were activated by 4 mM MgATP (added from a 200-mM stock titrated to pH 7.4 with NMg<sup>+</sup>). Patches from the animal pole of uninjected oocytes had a maximal ATP-induced pump current of  $0.55 \pm 0.15$  pA ( $n = 4$ ) in 25 mM Na<sup>+</sup><sub>i</sub> with NMg<sup>+</sup><sub>i</sub>.

Except for experiments with TEVC in Fig. 9 C, all measurements were performed at room temperature (22–23°C). Temperature control was performed with a TC10 controller (Dagan) as previously described (Stanley et al., 2015).

**Data analysis.** Data were analyzed with pClamp and Origin (OriginLab) software. The K<sup>+</sup><sub>o</sub> or Na<sup>+</sup><sub>i</sub> concentration dependence of pump currents were fitted with the Hill equation:

$$I = I_{\max}([S]^{n_H} / (K_{0.5}^{n_H} + [S]^{n_H})),$$

where  $I_{\max}$  is the current activated at saturating ion concentration  $S$ ,  $n_H$  is the Hill coefficient, and  $K_{0.5}$  is the ion concentration producing half-maximal current activation. Charge-voltage ( $Q$ - $V$ ) curves were fitted with a Boltzmann distribution:

$$Q = Q_{\text{hyp}} - Q_{\text{tot}} / (1 + \exp(z_q e (V - V_{1/2}) / kT)),$$

as described previously (Stanley et al., 2016), where  $Q_{\text{hyp}}$  is the charge moved with hyperpolarizing voltage pulses,  $Q_{\text{tot}}$  is the total charge moved,  $V_{1/2}$  is the center of the Boltzmann distribution on the voltage axis,  $z_q$  is the apparent valence of a charge that traverses the whole electric field,  $e$  is the elementary charge,  $k$  is the Boltzmann constant, and  $T$  is the absolute temperature; the slope factor is  $kT/ez_q$ . Individual  $Q$ - $V$  curves were normalized using the equation  $(Q - Q_{\text{hyp}})/Q_{\text{tot}}$  to eliminate variations caused by variable expression levels.

#### Radioactive ouabain binding and isotope uptake

**[<sup>3</sup>H]Ouabain binding.** After TEVC recording, each oocyte was bathed in NMg<sup>+</sup><sub>o</sub> with 10 μM [<sup>3</sup>H]ouabain for 10 min, washed three times with NMg<sup>+</sup><sub>o</sub> solution, placed into an individual scintillation vial, and mixed

with ScintiVerse (Fisher Scientific). Radioactivity was quantified using an LS6500 liquid scintillation counter (Beckman-Coulter). Radioactivity from [<sup>3</sup>H]ouabain binding to single uninjected oocytes was not distinguishable from background noise. Thus, endogenous binding was determined from the mean radioactivity detected in groups of five uninjected oocytes (each group placed into one scintillation tube;  $n = 15$ , three groups). Oocytes from one uninjected group were impaled with recording electrodes and clamped before binding measurements; [<sup>3</sup>H]ouabain binding to this group was identical to that measured in the other uninjected groups. Radioactive ouabain was added from a 100-μM stock in water made upon evaporating EtOH from 50 pmol [<sup>3</sup>H]ouabain (specific radioactivity 1.5 μCi; PerkinElmer).

**<sup>22</sup>Na<sup>+</sup> uptake.** Oocytes were removed from culture media, washed in NMg<sup>+</sup><sub>o</sub>, and incubated in a bath of Na<sup>+</sup><sub>o</sub> with <sup>22</sup>NaCl (specific activity: 416.56 mCi/mg; PerkinElmer) in the presence or absence of 100 μM ouabain for 2 h. 50 μM bumetanide (Sigma) was added to external solutions from a 50-mM stock in DMSO. Oocytes were washed four times in Na<sup>+</sup><sub>o</sub> with 100 μM ouabain and 50 μM bumetanide, transferred to individual scintillation tubes, and mixed with ScintiVerse for counting.

**<sup>86</sup>Rb uptake.** Oocytes taken from the incubator (non-loaded) or Na<sup>+</sup> loaded as described for TEVC recording were placed in Na<sup>+</sup><sub>o</sub> with 50 μM bumetanide in the presence or absence of 100 μM ouabain for 15 min. Oocytes were then incubated for 5 min (Na<sup>+</sup> loaded) or 15 min (non-loaded) in Na<sup>+</sup><sub>o</sub> with 50 μM bumetanide and 4.5 mM RbCl with added <sup>86</sup>RbCl (specific activity: 17.40 mCi/mg; PerkinElmer), with or without 100 μM ouabain. After incubation, oocytes were washed three times in Na<sup>+</sup><sub>o</sub> with 50 μM bumetanide, transferred to individual scintillation tubes, and mixed with ScintiVerse. Radioactivity was determined using a Tri-Carb 4810 TR Liquid Scintillation Analyzer (PerkinElmer). Time-controlled endogenous-pump-mediated uptake experiments using uninjected oocytes from the same batch were performed on the same day, under the same conditions.

#### Online supplemental material

Online supplemental material contains data of properties of human mutant pump currents not illustrated in the main figures. Figs. S1, S2, and S3 show ouabain unbinding kinetics from human pump mutants, the dose dependence for external K<sup>+</sup> activation of pump currents in the absence of external Na<sup>+</sup>, and the dose dependence of pump current activation by intracellular Na<sup>+</sup> activation without intracellular K<sup>+</sup>, respectively.

## RESULTS

### Effect of hyperaldosteronism mutants on *Xenopus* ouabain-resistant pumps

To evaluate the functional consequences of the previously described hyperaldosteronism-associated mutants (L104R, V332G, delF100-L104, and EETA963S), we introduced them into the ouabain-resistant *Xenopus* RD- $\alpha 1$  subunit (human  $\alpha 1$  numbering is used throughout for consistency; see Materials and methods), co-injected them in *Xenopus* oocytes with *Xenopus*  $\beta 3$ , and studied their function 2–4 d after their injection (Fig. 2). Expression of these ouabain-resistant mutants ( $\sim 100$   $\mu\text{M}$   $\text{IC}_{50}$ ) allows for the inhibition of endogenous pumps by preincubation with 10  $\mu\text{M}$  ouabain (Canezza et al., 1992; Yaragatupalli et al., 2009; Materials and methods) while leaving the signal from exogenous ouabain-resistant pumps unaltered. A representative recording from an oocyte expressing the *Xenopus* RD template (Fig. 2 A) shows activation of outward current (caused by canonical  $3\text{Na}^+/2\text{K}^+$  exchange) in response to application of  $\text{K}^+$  in 125  $\text{NMG}^+$  ( $\text{NMG}^+$  solution) and the absence of inward current at  $-50$  mV in 125 mM  $\text{Na}^+$  ( $\text{Na}^+$  solution), as we have previously documented (Yaragatupalli et al., 2009; Ratheal et al., 2010; Mitchell et al., 2014).  $\text{K}^+$  failed to induce outward current when applied in  $\text{NMG}^+$  solution on an oocyte expressing *Xenopus* RD-L104R- $\alpha 1$  pumps (Fig. 2 B, L106R in *Xenopus* numbering). In addition, substitution of  $\text{NMG}^+$  with  $\text{Na}^+$  induced a relatively large inward current that was only partially inhibited by 10 mM ouabain. Vertical current deflections in the traces correspond to 100 ms-long pulses used to obtain the I-V relationships. The currents at the end of such pulses in the presence of ouabain were subtracted from the currents in the absence of inhibitor to obtain the Na/K pump-mediated current, plotted against voltage in the I-V curves (Fig. 2 C). The inward currents observed in  $\text{Na}^+$  solution at negative voltages, and their reduction upon substitution with  $\text{NMG}^+$ , are consistent with previous observations in oocytes expressing human  $\alpha 1\beta 1$  pumps with the same ouabain resistance-conferring mutations (Azizan et al., 2013).

RD pumps lack inward currents in the presence of  $\text{Na}^+$ , but they transport inward leak currents when  $\text{Na}^+$  and  $\text{K}^+$  are absent from the external solution (Yaragatupalli et al., 2009; Ratheal et al., 2010; Mitchell et al., 2014). Vedovato and Gadsby (2014) showed that this leak through “normal” ouabain-resistant *Xenopus* pumps is ablated by the mutation D933N (D935N in *Xenopus* numbering), a critical residue for coordination of  $\text{Na}^+$  at the  $\text{Na}^+$ -exclusive ion-binding site III (Kanai et al., 2013), suggesting that  $\text{H}^+$  ions transit through site III. Kopeck et al. (2014) specifically proposed that the ions “leaking” through the multiply substituted EETA963S mutant transit site III, similar to wild type, whereas

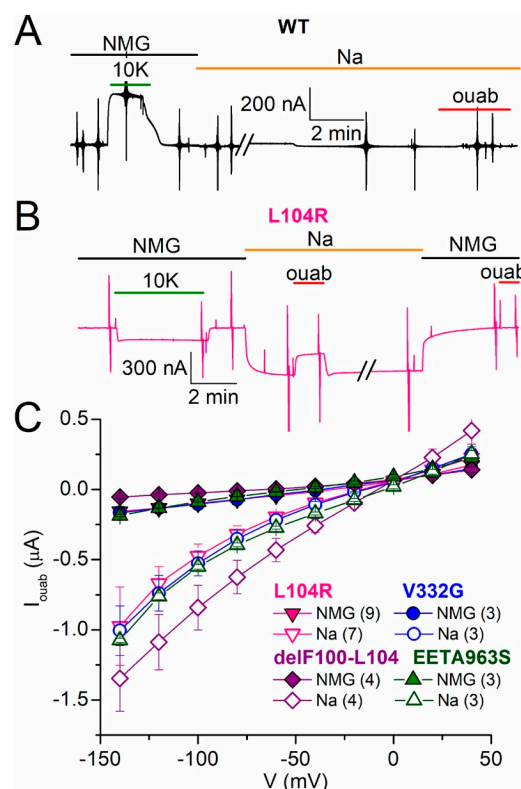


**Figure 2. Hyperaldosteronism mutations in *Xenopus* Na/K pumps.** (A) TEVC recording at  $-50$  mV from a  $\text{Na}^+$ -loaded oocyte expressing wild type. Application of 10 mM  $\text{K}^+$  in  $\text{NMG}^+$  stimulated outward current. There is zero ouabain (ouab)-sensitive steady-state current in  $\text{Na}^+$  alone. (B) A similar TEVC recording from an oocyte expressing L104R, 3 d after cRNA injection.  $\text{K}^+$ -induced outward current was absent, and switching from  $\text{NMG}^+$  to  $\text{Na}^+$  induced an inward current that was partially inhibited by perfusion of 10 mM ouabain. Vertical deflections along the current trace represent 100-ms voltage pulses to obtain I-V curves. (C) Mean ouabain-sensitive I-V plots measured in  $\text{NMG}^+$  (filled symbols) and in  $\text{Na}^+$  (open symbols), 3–4 d after injection, from oocytes expressing L104R (down triangles), V332G (circles), delF100-L104 (diamonds), and EETA963S (up triangles). Number of experiments is indicated in parentheses. Error bars represent SEM.

L104R, V332G, and delF100-L104 open a distinct ion pathway in the vicinity of site II. To test whether the inward currents through hyperaldosteronism mutants traverse pathways separate from the wild-type passive  $\text{H}^+$  current, we introduced D933N into ouabain-resistant *Xenopus* RD- $\alpha 1$  containing the aforementioned hyperaldosteronism mutations and measured ouabain-sensitive currents in the presence and absence of  $\text{Na}^+$  (Fig. 3). Fig. 3 A illustrates the current, at  $-50$  mV, from an oocyte expressing RD-V332G/D933N. (Note that switching to  $\text{Na}^+$  induced an inward current partially inhibited by 10 mM ouabain.) The ouabain-sensitive I-V curves show significant leak current for the double mutants RD-L104R/D933N, RD-V332G/D933N, and RD-delF100-L104/D933N but a largely attenuated current through RD-EETA963S/D933N (Fig. 3 B), consis-

tent with the leak pathway through EETA963S crossing site III and the presence of an independent pathway for the other mutants. A Western blot from plasma membrane of oocytes injected with RD-EETA963S/D933N confirmed expression of the mutant pumps (Fig. 3 C).

The currents induced by  $\text{Na}^+$  in Figs. 2 and 3 appeared to be only partially inhibited by ouabain and quickly returned to their steady-state levels after ouabain removal, suggesting that at least some hyperaldosteronism mutations reduce ouabain affinity by increasing the unbinding rate. Thus, the experiments with RD-EETA963S/D933N could be misleading if ouabain affinity is further reduced by D933N; it is also difficult to fully assess the alterations induced by these mutations if they are introduced in the ouabain-resistant RD- $\alpha 1$  background. Therefore, we introduced EETA963S and EETA963S/D933N in the highly ouabain-sensitive human  $\alpha 1$  template ( $\text{IC}_{50}$  5–20 nM; Crambert et al., 2000) to test whether large inward currents are observed in  $\text{Na}^+$ -loaded oocytes not preincubated with ouabain (Fig. 4).

#### Effect of hyperaldosteronism mutations on human Na/K pumps

An alternative to using ouabain-resistant pumps in oocytes is to overexpress ouabain-sensitive pumps. This approach avoids complications regarding the functional consequences of ouabain-resistant mutations, but it requires that the expression levels of exogenous pumps be much higher than endogenous levels (Stanley et al., 2015). A representative current recording from an uninjected oocyte (Fig. 4 A, left), in which ouabain was excluded from the  $\text{Na}^+$ -loading solution (see Materials and methods), shows reversible activation of a small outward current in response to application of 3 mM  $\text{K}^+$  ( $23 \pm 1$  nA,  $n = 4$ ). Replacement of  $\text{NMG}^+$  with  $\text{Na}^+$  or application of 1 mM ouabain in  $\text{Na}^+$  were without effect on baseline current. The expanded time scale of the ouabain-sensitive signal in  $\text{Na}^+$  (Fig. 4 A, right, current without inhibitor minus current in ouabain), elicited by pulses from  $-140$  to  $40$  mV in 20-mV increments, illustrate the presence of small transient currents in uninjected oocytes. These currents represent the transition between  $\text{E1P}(3\text{Na}) \leftrightarrow \text{E2P}$  when the equilibrium is perturbed by a change in voltage (without net steady-state ion transport in normal pumps). The integrals of these current traces are used to construct Q-V curves (e.g., Fig. 4 E). Fig. 4 B shows Na/K pump-mediated signals seen in a representative current recording from an oocyte expressing human wild-type  $\alpha 1\beta 1$  pumps (an outward current in response to application of  $\text{K}^+$  is shown on the left, and ouabain-sensitive transients in  $\text{Na}^+$  are shown on the right). Note the absence of steady-state ouabain-sensitive current in  $\text{Na}^+$  (zero current indicated with gray dashed line). The  $\sim 20$ -fold difference in observed current amplitude between the traces in Fig. 4 (A and B) is consistent with a previous study (Stanley et al., 2015).

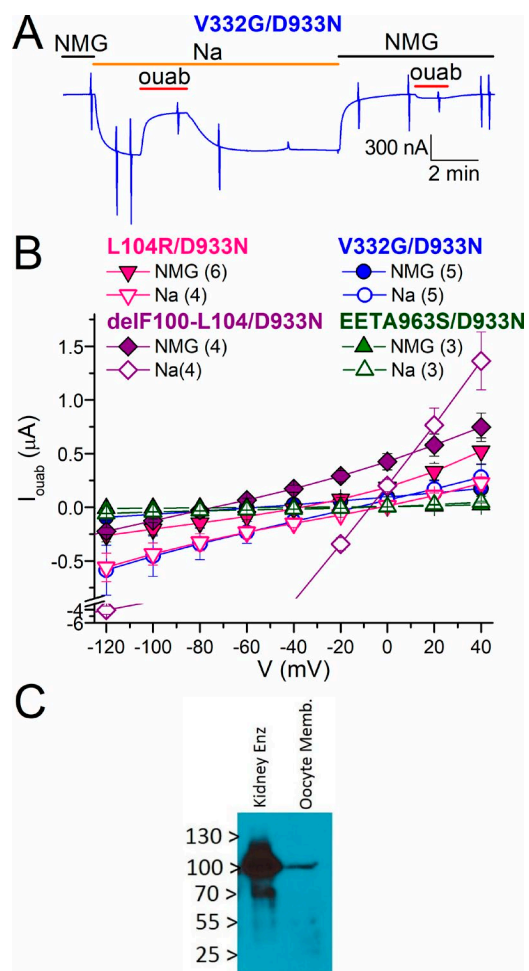


**Figure 3. Effect of D933N on the mutants' leak currents.** (A) Continuous TEVC recording at  $-50$  mV from an oocyte expressing V332G/D933N. (B) Mean  $I_{\text{ouab}}$  in  $\text{NMG}^+$  (filled symbols) and  $\text{Na}^+$  (open symbols) for double mutants L104R/D933N (down triangles), V332G/D933N (circles), delF100-L104/D933N (diamonds), and EETA963S/D933N (up triangles), recorded 3–4 d after injection. Note axis break at negative currents caused by larger currents in oocytes expressing delF100-L104/D933N. The number of experiments is indicated in parentheses. Error bars represent SEM. (C) Western blot of protein recognized by the Anti-KETYY antibody targeting the C-terminal end of the Na/K-ATPase. Left lane shows purified sheep kidney enzyme (0.5  $\mu\text{g}$  total protein) and a membrane preparation from 25 oocytes injected with *Xenopus* RD- $\alpha 1$ -EETA963S/D933N cRNA (20  $\mu\text{g}$  total protein). Bands at  $\sim 110$  kD (the approximate mass of the Na/K-ATPase  $\alpha$ -subunit) are visible for both samples.

Representative traces from oocytes expressing EETA963S (Fig. 4 C) or EETA963S/D933N (Fig. 4 D) held at  $-50$  mV illustrate that these mutant pumps show  $\text{K}^+$ -induced currents (left traces) with amplitudes between those observed in uninjected and wild-type-injected oocytes. Both mutants produce larger transient currents (right traces) than uninjected oocytes, with altered kinetics compared with wild-type-injected oocytes. Steady-state currents were present in EETA963S but nearly absent in EETA963S/D933N, consistent with



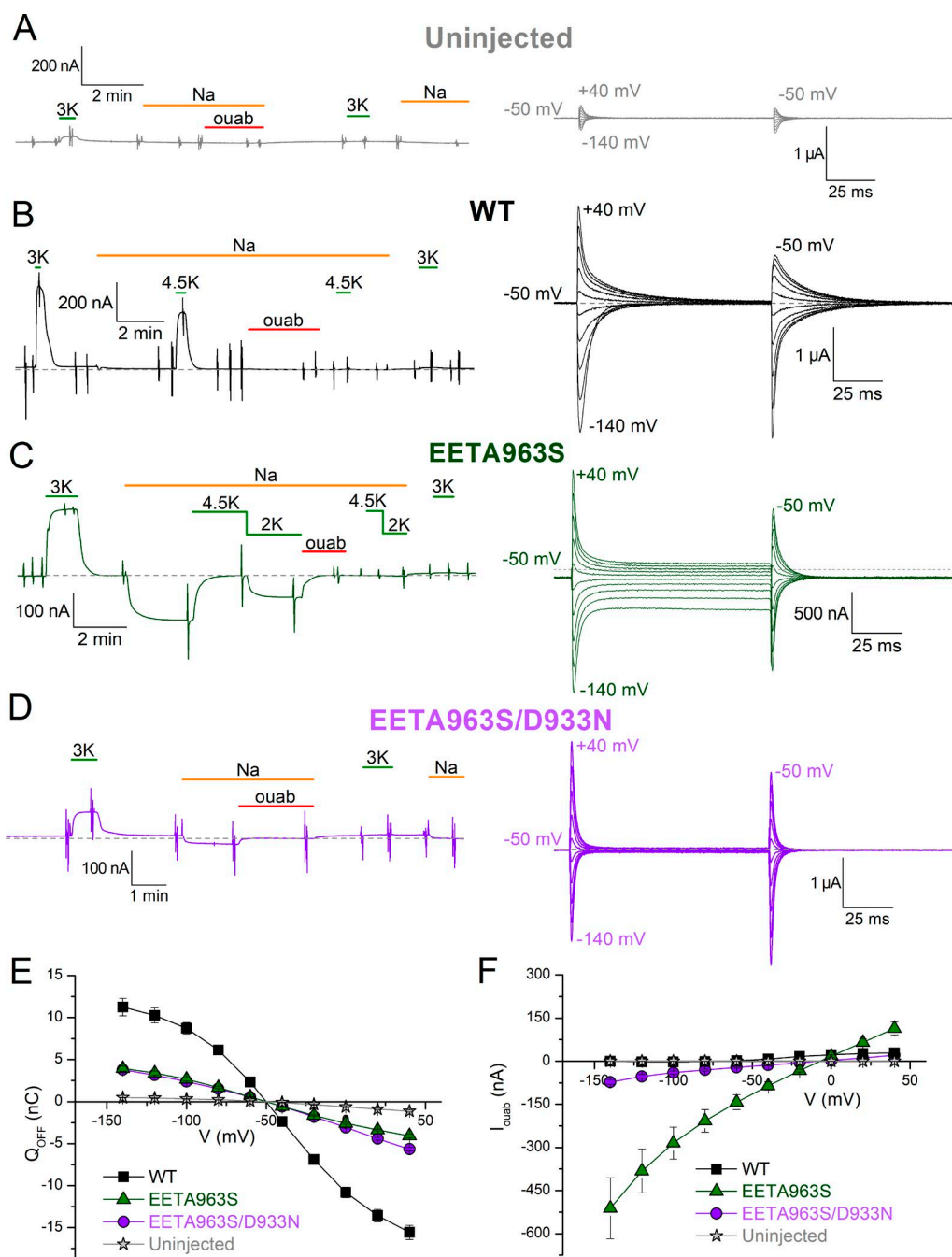


**Figure 4. Wild-type, EETA963S, and EETA963/D933N human pumps.** (A–D) Representative current recordings from  $\text{Na}^+$ -loaded oocytes that were uninjected (A) or injected with human Na/K pump cRNA encoding wild type (B), EETA963S (C), or EETA963S/D933N (D). Left traces show a continuous recording illustrating the effect of several experimental maneuvers on holding current at  $-50$  mV. In all four cases, initial application of  $\text{K}^+$  in  $\text{NMG}^+$  activated outward current. Substitution of  $\text{NMG}^+$  with  $\text{Na}^+$  induced inward current only in EETA963S. For wild type and EETA963S,  $4.5$  mM  $\text{K}^+$  applied in  $\text{Na}^+$  activated a large outward current. Note that after a 2-min application of  $1$  mM ouabain, there is no response to subsequent application of  $\text{K}^+$  in all cases, and that the inward current through EETA963S is irreversibly blocked. Right traces show ouabain-sensitive currents measured in  $\text{Na}^+$  in the same oocytes shown on the left, evoked by application of 100-ms-long pulses to voltages between  $-140$  and  $40$  mV in  $20$ -mV increments. Gray dashed lines indicate zero-current level. (E) Mean  $Q$ -V curves from uninjected (stars,  $n = 7$ ), wild-type-injected (squares,  $n = 5$ ), EETA963S-injected (up triangle,  $n = 4$ ), and EETA963S/D933N-injected (circles,  $n = 5$ ) oocytes. (F) Mean ouabain-sensitive, steady-state currents in  $\text{Na}^+$  for same conditions and oocytes in E. Error bars represent SEM.

the site III mutation D933N disrupting the leak pathway. The mean Q-V curves from oocytes expressing uninjected, wild type, EETA963S, and EETA963S/D933N (Fig. 4 E) demonstrate robust expression of these three human pump variants. The mean ouabain-sensitive steady-state currents (Fig. 4 F) were much smaller in oocytes expressing EETA963S/D933N than in oocytes expressing EETA963S, similar to the results with *Xenopus* RD- $\alpha$ 1 in Fig. 3.

It must be noted that the inward current amplitude observed in oocytes expressing all "leaky" mutants in the physiologically relevant range (between  $-40$  and  $-80$  mV; Figs. 3 B and 4 F) have amplitudes similar to the macroscopic outward currents observed in oocytes expressing the RD- $\alpha$ 1 $\beta$ 3 or  $\alpha$ 1 $\beta$ 1 pumps (typically a few hundred nanoamperes). Because the normal wild-type outward Na/K pump current is known to contribute minimally to setting the resting membrane potential of most cells, it is doubtful that inwardly directed currents of similar amplitude constitute a gain-of-function capable of significant membrane depolarizations. Furthermore, for EETA963S (Fig. 4 C), the large amount of current induced by applying  $4.5$  mM  $K^+$  in  $Na^+$  solution at  $-50$  mV (i.e., extracellular physiological conditions) completely cancels out the inward leak current observed when  $Na^+$  was the only monovalent cation in the solution. This observation makes it extremely unlikely that this mutant's passive inward current induces depolarization in vivo (see Discussion).

Because important quantitative nuances regarding current amplitudes may not be directly translated from *Xenopus* RD- $\alpha$ 1 pumps to the pumps mutated in hyperaldosteronism patients, we evaluated the consequences of also introducing L104R, V332G, and delF100-L104 in human  $\alpha$ 1 $\beta$ 1 pumps (Figs. 5 and 6).

Representative current recordings (at  $-50$  mV) from oocytes expressing the human  $\alpha$ 1 mutants L104R (Fig. 5 A), V332G (Fig. 5 B), and delF100-L104 (Fig. 5 C) illustrate their distinct responses to  $K^+$  application in NMG $^+$ ; although L104R and V332G showed smaller outward currents than wild-type-injected oocytes (also, it is likely that endogenous pumps contribute significantly to these small outward currents), delF100-L104-expressing oocytes displayed a small inward current (due to inhibition of outward current). Substituting NMG $^+$  with  $Na^+$  solution induced an inward current in all three mutants. This inward current was partially reduced by  $K^+$  application ( $2$  and  $4.5$  mM) and abolished by  $1$  mM ouabain. The ouabain-sensitive signals in  $Na^+$  solution are shown with a faster time base on the right (Fig. 5). Oocytes expressing either of the three mutants presented varying amplitudes of steady-state currents at all voltages (dashed lines indicate zero current level). A significantly larger inward current was observed for delF100-L104, which made it nec-

essary to take measurements  $2$  or  $3$  d after injection (instead of the typical  $4$ – $5$  d).

Ouabain-sensitive I-V relationships of each hyperaldosteronism mutant in different external solutions were compared with those in wild-type pumps (Fig. 6). The wild-type human pump (Fig. 6 A) presents robust outward current in the presence of  $K^+$  in both NMG $^+$  and  $Na^+$ . It also displays ouabain-sensitive inward leak currents at very negative voltages when NMG $^+$  is the only monovalent cation in the solution; this inward current is blocked by  $Na^+$ . For L104R, V332G, and delF100-L104 (Figs. 6, B–D), pumping is drastically impaired; very small ouabain-sensitive currents appear to be activated by  $3$  mM  $K^+$  in NMG $^+$  (again probably carried by endogenous pumps). The presence of  $K^+$  partially inhibits leak currents in the presence of  $Na^+$  in oocytes expressing V332G and delF100-L104 but may not be able to induce electrogenic transport, as previously reported (Azizan et al., 2013). Also in agreement with the findings of Azizan et al. (2013), we observed electrogenic pumping from EETA963S, which displays robust ouabain-sensitive outward current in the presence of  $3$  mM  $K^+$  and NMG $^+$  (Fig. 6 E; see also Fig. 4 C). The outward current induced by  $4.5$  mM  $K^+$  in the presence of  $Na^+$  counters the inward current observed in  $Na^+$  alone, resulting in a ouabain-sensitive current that reverses at approximately  $-50$  mV in the presence of both ions.

To determine the charge carrier in each human mutant, we measured the effect of replacing  $Na^+$  with NMG $^+$  on the reversal potential of ouabain-sensitive current. The insets in Fig. 6 (B–E) show an expanded axis scale of the plots in the presence of  $125$  mM  $Na^+$  or  $125$  mM NMG $^+$ . The mean reversal potential of ouabain-sensitive current (Fig. 6 F, bar graph; summarized in Table 1) demonstrates that although all mutants allow  $Na^+$  inflow, only the current in delF100-L104 is almost exclusively carried by  $Na^+$  at pH  $7.6$ . Thus, the electrophysiological characteristics of all four mutants in ouabain-sensitive human pumps are congruent with previously reported results for the same mutations incorporated in human pumps with ouabain resistance-conferring mutations (Azizan et al., 2013).

#### Turnover rate of wild-type human Na/K pump current

It is obvious from the aforementioned measurements that only delF100-L104 pumps have inward currents that are much larger at negative voltages than the outward current from wild-type pumps. The total current in an oocyte depends on the expression level, which can be altered by inconsistencies in the cRNA quality, among other hard-to-control variables. Thus, the only way to test whether the inward currents are large enough to account for the proposed gain-of-function is to measure the currents and independently count the number of



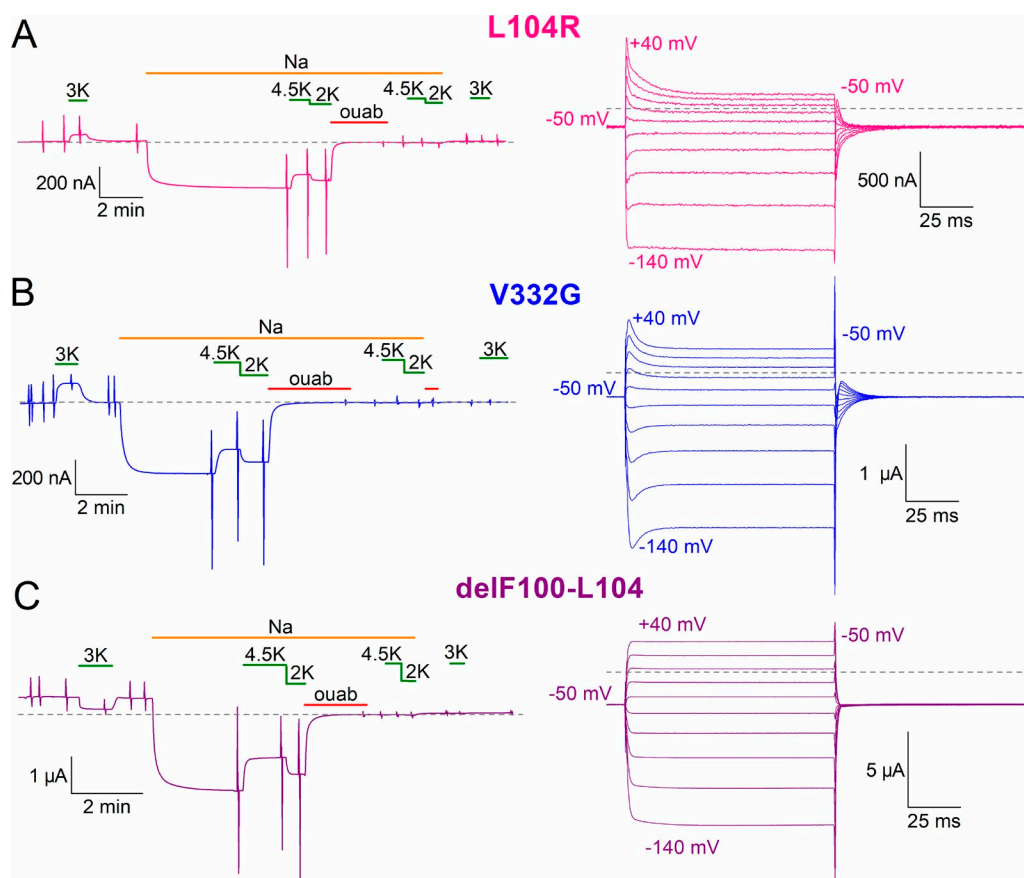


Figure 5. **L104R, V332G, and delF100-L104 human pumps.** (A–C) Representative current recordings from  $\text{Na}^+$ -loaded oocytes, expressing L104R (A), V332G (B), and delF100-L104 (C). Left traces show the effect on holding current at  $-50$  mV of the same experimental maneuvers shown in Fig. 4 C. Right traces show voltage pulse-evoked ouabain-sensitive currents in  $\text{Na}^+$  solution from the same oocytes shown on the left. Gray dashed lines indicate zero-current level.

pumps in the same oocyte to obtain the turnover rate of the transporters.

For wild-type pumps, the number of Na/K pump molecules in the plasma membrane may be determined in two ways: (1) by directly counting the number of ouabain-binding sites with  $[^3\text{H}]$ ouabain (ouabain binds to the pump with a 1:1 stoichiometry) or (2) by measuring the total ouabain-sensitive transient charge moved in the same oocyte in the presence of  $\text{Na}^+$  and absence of  $\text{K}^+$  upon voltage pulses like those shown in Fig. 4 A (right). Although the second method, based on the assumption of one total elementary charge moved per pump, is often preferred because of its cost efficiency and simplicity (Tavraz et al., 2008; Vedovato and Gadsby, 2014; Stanley et al., 2015), the distorted transient currents concomitant to steady-state currents (Fig. 4 C; and Fig. 5, A–C) preclude using this method for the leaky mutants. Thus, we measured the steady-state current and  $[^3\text{H}]$ ouabain binding in the same oocytes to estimate the turnover rate ( $t/o$ ; Fig. 7).

Fig. 7 A shows a representative oocyte in which application of  $3$  mM  $\text{K}^+$  in  $\text{NMG}^+$  activated  $760$  nA of

outward pump current when applied  $5$  d after injection ( $3$  mM  $\text{K}^+$  activated  $443 \pm 42$  nA,  $n = 17$ ). Upon withdrawal of  $\text{K}^+$ , the current returned to the baseline and the oocyte was carefully removed from the recording chamber and incubated in  $10$   $\mu\text{M}$   $[^3\text{H}]$ ouabain for  $10$  min. After three washes, the oocyte was placed in an individual scintillation vial, where we measured  $225$  fmol bound ouabain ( $146 \pm 13$  fmol ouabain bound to the same  $17$  oocytes). In comparison, uninjected oocytes bound  $9.0 \pm 1.0$  fmol ( $n = 15$ ), representing unspecific and endogenous pump binding. Thus, because of exogenous human pump overexpression, there is a minimal contribution from endogenous pumps to the pump current (see Fig. 4 above; Stanley et al., 2015) or ouabain-binding signals. For each oocyte, the steady-state  $\text{K}^+$ -induced currents were converted to moles of charge per second ( $F = 96,485$  C $\cdot\text{mol}^{-1}$ ) and divided by the moles of  $[^3\text{H}]$ ouabain bound to the oocyte, yielding a mean rate of outward charge transport per pump  $t/o_{\text{out}} = 32.0 \pm 1.5$  s $^{-1}$  (Table 2) nearly identical to the  $t/o_{\text{out}} = 36.3 \pm 8.5$  s $^{-1}$  previously reported by Crambert et al. (2000) using the same method.

Table 1. Reversal potential ( $V_{REV}$ ) of ouabain-sensitive leak currents produced by human Na/K pump  $\alpha 1$ -mutants in  $\text{NMG}^+$  or  $\text{Na}^+$  in oocytes

| Mutant       | n | $V_{REV}$ in $\text{NMG}^+$ | $V_{REV}$ in $\text{Na}^+$ |
|--------------|---|-----------------------------|----------------------------|
|              |   | mV                          | mV                         |
| L104R        | 5 | $-51.0 \pm 1.7$             | $-10.2 \pm 1.0$            |
| V332G        | 5 | $-50.1 \pm 1.4$             | $-8.9 \pm 1.0$             |
| delF100-L104 | 5 | $-103.6 \pm 1.3$            | $-7.2 \pm 0.9$             |
| EETA963S     | 4 | $-37.7 \pm 5.3$             | $-6.9 \pm 0.7$             |

Reversal potential ( $V_{REV}$ ) values are mean  $\pm$  SEM. n, number of oocytes.

### Inward current turnover rate of hyperaldosteronism mutant pumps

Steady-state inward current through each leaky pump was measured as the current induced by switching from  $\text{NMG}^+$  solution to  $\text{Na}^+$  solution at  $-50$  mV, which is nearly identical to ouabain-sensitive inward current

(see Figs. 4 C and 5 above). A representative trace from an oocyte expressing L104R (Fig. 7 B) shows reversible activation of a 694 nA inward current upon switching from  $\text{NMG}^+$  to  $\text{Na}^+$ . As described above for wild-type pumps, the oocyte was removed from the recording chamber, incubated in  $[^3\text{H}]$ ouabain, washed, and placed in a scintillation tube, where 289 fmol ouabain was measured. Although the rate of ouabain unbinding in human pumps was increased by the hyperaldosteronism mutations, as observed earlier with *Xenopus* pumps, more than 98% of pumps remained bound to ouabain after 2 min, the maximum time needed to wash the oocyte before transferring it to the scintillation vial (Fig. S1; see also Figs. 4 C and 5).

Oocytes expressing mutant pumps also bound large ouabain quantities (Table 2) while presenting inward currents that were similar in amplitude to the outward pump currents produced by wild-type pumps. Oocytes

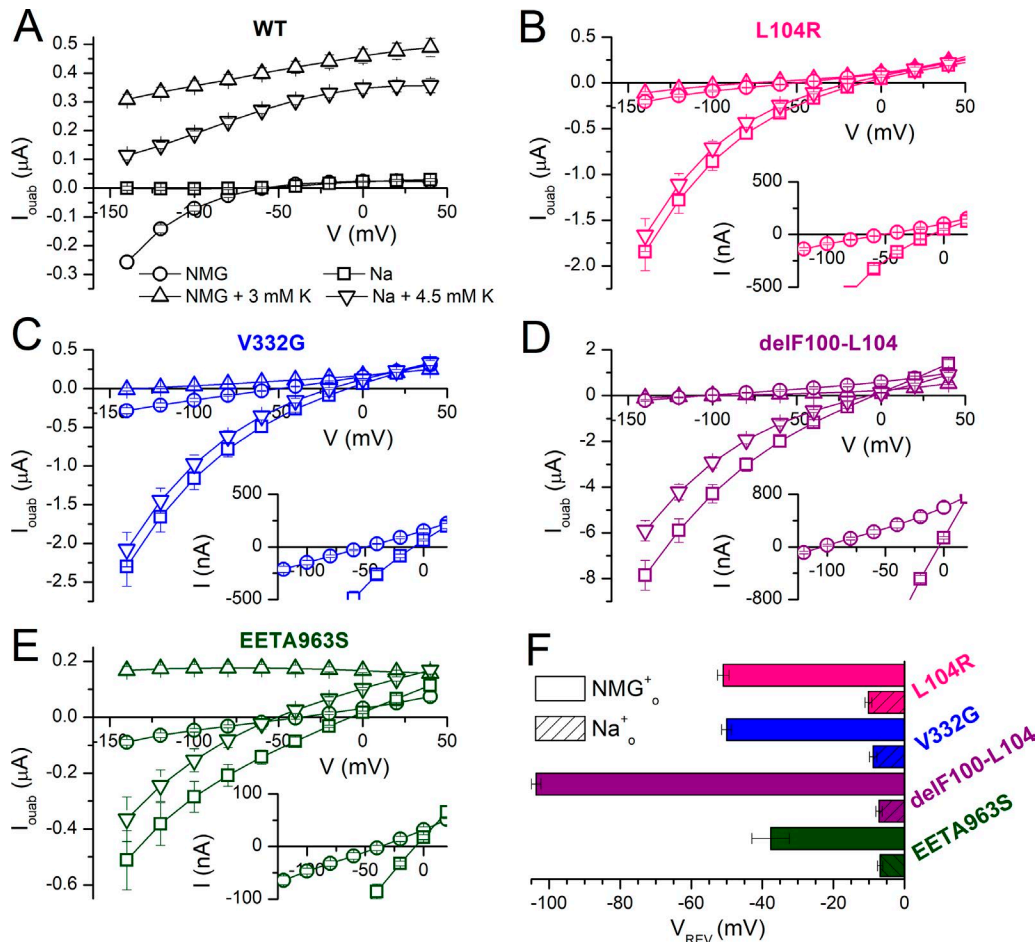


Figure 6. Ouabain-sensitive currents in wild-type and mutant human Na/K pumps. (A–E) Mean ouabain-sensitive I–V plots in different ionic conditions from oocytes expressing wild-type ( $n = 5$ ; A), L104R ( $n = 5$ ; B), V332G ( $n = 5$ ; C), delF100-L104 ( $n = 5$ ; D), and EETA963S ( $n = 4$ ; E) pumps, recorded 2–4 d after injection in experiments similar to those in Figs. 4 and 5. Shown are ouabain-sensitive currents in  $\text{NMG}^+$  (circles),  $\text{NMG}^+$  + 3 mM  $\text{K}^+$  (up triangles),  $\text{Na}^+$  (squares), and  $\text{Na}^+$  + 4.5 mM  $\text{K}^+$  (down triangles; symbol key in A). The insets in B–D show a zoomed-in view of the axes to illustrate the shift in reversal potential ( $V_{REV}$ ) when  $\text{Na}^+$  was replaced with  $\text{NMG}^+$ . (F) Mean reversal potential of ouabain-sensitive currents in  $\text{NMG}^+$  (solid bars) and  $\text{Na}^+$  (striped bars). Error bars represent SEM.

Table 2. [<sup>3</sup>H]Ouabain-bound and maximal turnover rates of outward current produced by wild-type pumps with 3 mM K<sup>+</sup><sub>o</sub> in NMG<sup>+</sup><sub>o</sub> (t/o<sub>out</sub>) or of inward currents produced by mutant pumps (t/o<sub>in</sub>) in Na<sup>+</sup><sub>o</sub> without K<sup>+</sup><sub>o</sub>, measured at −50 mV

| Mutant       | n  | [ <sup>3</sup> H]Ouabain<br>fmol | t/o <sub>out</sub> (s <sup>−1</sup> )<br>3 K <sup>+</sup> <sub>o</sub> | t/o <sub>in</sub> (s <sup>−1</sup> )<br>Na <sup>+</sup> <sub>o</sub> |
|--------------|----|----------------------------------|--|--|
|              |    |                                  |  |  |
| Wild type    | 17 | 146 ± 13                         | 32.0 ± 1.5   |  |
| L104R        | 14 | 317 ± 32                         |  | 22.8 ± 1.9   |
| V332G        | 12 | 220 ± 9                          |  | 63.4 ± 6.2   |
| delF100-L104 | 4  | 62.4 ± 4.7                       |  | 522 ± 120  |
| EETA963S     | 10 | 314 ± 19                         |  | 19.7 ± 1.5   |

n, number of oocytes.

expressing the deletion mutant (delF100-L104) consistently deteriorated and could not be voltage-clamped beyond the third day after injection. Thus, oocytes expressing delF100-L104 were studied 2–3 d after injections, when the total bound ouabain was only 62.4 ± 4.7 fmol (n = 4). Fortunately, because endogenous pumps lack inward current in Na<sup>+</sup><sub>o</sub>, the mean background binding (9 fmol) could be subtracted from the ouabain bound to each oocyte expressing human Na/K pump mutants, even at lower expression levels, to obtain accurate turnover rates for inward current. Table 2 summarizes the turnover rate of Na<sup>+</sup><sub>o</sub>-induced inward currents (t/o<sub>in</sub>) in mutant-injected oocytes and for Na/K pump current (t/o<sub>out</sub>) in wild-type-injected oocytes at −50 mV.

Evidently, the maximal turnover rate of wild-type pumping in the presence of K<sup>+</sup><sub>o</sub> is faster than the maximal rate of charge inflow through L104R and EETA963S but 2- and 16-fold slower than the rate of charge inflow through V332G and delF100-L104, respectively (Fig. 7 C and Table 2). These maximal turnover rates make it unlikely for some mutations (e.g., L104R) to have a large enough inward leak current capable of significantly depolarizing the membrane of aldosterone-producing adenomas. In some cases (e.g., EETA963S), the real leak value, corrected for the effect of K<sup>+</sup><sub>o</sub>, is further reduced (see Discussion).

### Electrophysiological evaluation of G99R

Recently, Williams et al. (2014) identified another Na/K pump mutant in a patient with an aldosterone-producing adenoma, where Gly99 on TM1 was mutated to Arg. Due in part to its location within the “hotspot region” near site II, this mutation was predicted to behave similar to the other TM1 and TM4 mutants (Williams et al., 2014; Azizan and Brown, 2016). We used TEVC (Figs. 8 and 9) and patch clamp (Fig. 10) to characterize the human α1-G99Rβ1 Na/K pump mutant expressed in *Xenopus* oocytes.

The recordings at a slow time base illustrate representative experiments where outward currents were activated by step increments in K<sup>+</sup><sub>o</sub> concentration applied in Na<sup>+</sup><sub>o</sub> over an oocyte expressing wild-type (Fig. 8 A)

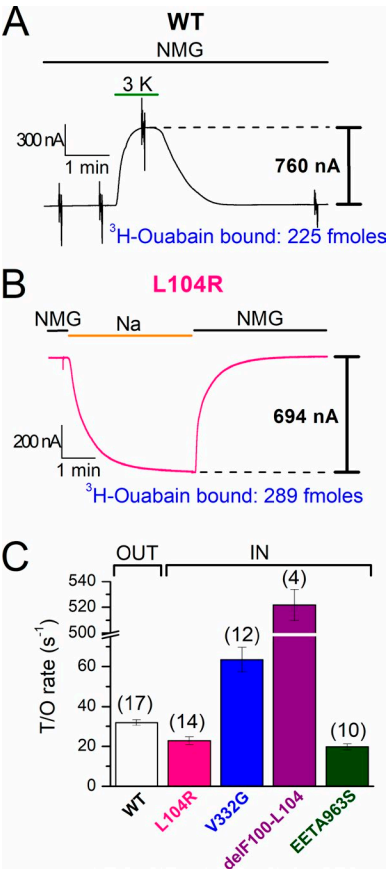
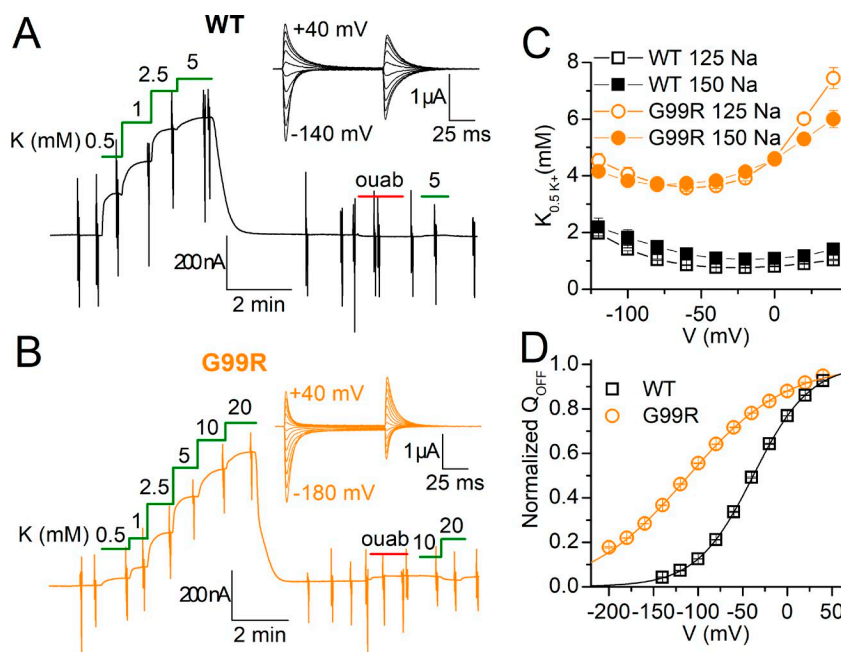


Figure 7. Turnover rates of wild-type and mutant human Na/K pumps. (A) Representative recording from an oocyte expressing wild-type pumps, held at −50 mV, in which application of 3 mM K<sup>+</sup><sub>o</sub> in NMG<sup>+</sup><sub>o</sub> induced outward current. (B) Representative recording from an oocyte expressing L104R pumps in which replacing NMG<sup>+</sup><sub>o</sub> with Na<sup>+</sup><sub>o</sub> solution induced inward current. The quantity of [<sup>3</sup>H]ouabain bound to the oocytes in A and B is also indicated. (C) Bar graph showing mean turnover rates (moles of charge per second/moles of [<sup>3</sup>H]ouabain bound; i.e., s<sup>−1</sup>) measured in individual oocytes, for the outward current (bracketed as “OUT”) in oocytes expressing wild type (n = 17) and for the Na<sup>+</sup><sub>o</sub>-induced inward current (bracketed as “IN”) in oocytes expressing L104R, V332G, delF100-L104, and EETA963S. Measurements were performed 4–5 d after injection, except for delF100-L104, which was performed 3 d after injection because of large currents. Note the break along the y axis. The number of experiments is indicated in parentheses. Error bars represent SEM.

and another expressing G99R pumps (Fig. 8 B). Perfusion of K<sup>+</sup><sub>o</sub> after a 2-min application of 1 mM ouabain failed to stimulate current. Thus, G99R, like wild type, is an electrogenic pump that lacks inward currents in Na<sup>+</sup><sub>o</sub> solution (Fig. 8, A and B, inset). A Hill equation was fitted to the concentration dependence of the K<sup>+</sup><sub>o</sub>-induced current at all voltages and the mean K<sub>0.5</sub> plotted as a function of voltage showing an approximately fourfold reduction in apparent affinity for K<sup>+</sup><sub>o</sub> (Fig. 8 C, open symbols). Similar curves were obtained under more physiological external conditions, i.e.,





**Figure 8.  $K^+$  dependence of wild-type and G99R pumps.** (A and B) TEVC recordings at  $-50$  mV from representative oocytes 4–5 d after injection with wild-type (A) or G99R (B) cRNA. Application of  $K^+$  in  $Na^+$  solution stimulated outward current in a  $[K^+]_o$ -dependent manner. Addition of 10 and 20 mM  $K^+$  did not activate outward current after application and withdrawal of 1 mM ouabain. Insets in A and B are the expanded time-scale ouabain-sensitive transient currents in  $Na^+$  upon 100-ms voltage steps from  $-50$  mV. (C) Mean  $K_{0.5}$  for  $K^+$ , as a function of voltage, for wild type (squares) and G99R (circles), measured in 125 mM  $Na^+$  (open symbols) or 150 mM  $Na^+$  (solid symbols). Wild type at 125 mM  $Na^+$  ( $n = 6$ ) and at 150 mM  $Na^+$  ( $n = 4$ ); G99R at 125 mM  $Na^+$  ( $n = 3$ ) and at 150 mM  $Na^+$  ( $n = 8$ ). (D) Mean normalized  $Q_{off}$ -V curves in 125 mM  $Na^+$  for wild type (squares,  $n = 7$ ) and G99R (circles,  $n = 6$ ). Line plots represent a Boltzmann with parameters in the text. Error bars in C and D are SEM, smaller than the symbols for most data points.

150 mM  $Na^+_o$ , at pH 7.4 (Fig. 8 C, solid symbols). We also performed additional dose–response experiments for  $K^+_o$  without  $Na^+_o$  (in  $NaMG^+_o$ ; Fig. S2), which showed a reduced apparent affinity for  $K^+_o$  (three- to eightfold, depending on voltage) for G99R. The turnover rate measured in five G99R-injected oocytes in  $NaMG^+_o$  with 3 mM  $K^+_o$  (90% maximal) was  $t/o_{out} = 24.0 \pm 2.8$  (mean bound ouabain,  $193 \pm 29$  fmol).

To evaluate the effect of G99R on  $Na^+_o$  interaction in the absence of the competitor  $K^+_o$ , we measured the ouabain-sensitive transient currents in 125 mM  $Na^+_o$  (Fig. 8, A and B, inset). The integrals of these transients give the charge moved during the voltage pulse, which was plotted against the voltage (Fig. 8 D) in the so-called  $Q$ -V curves normally described by a Boltzmann distribution (Materials and methods). The mean parameters rendered from the fits to the individual experiments averaged in Fig. 8 D were  $V_{1/2} = -38 \pm 1$  mV and slope factor  $kT/ez_q = 32 \pm 1$  mV ( $n = 7$ ) for wild type, and  $V_{1/2} = -109 \pm 2$  mV;  $kT/ez_q = 54 \pm 1$  mV ( $n = 6$ ) for G99R, consistent with the mutant having an approximately eightfold decrease in overall  $Na^+_o$  apparent affinity; a 25-mV shift of the  $V_{1/2}$  corresponds to a two-fold change in external  $Na^+_o$  concentration (Holmgren et al., 2000; Holmgren and Rakowski, 2006) or twofold change in overall external  $Na^+$  affinity (Li et al., 2005; Yaragatupalli et al., 2009; Meier et al., 2010; Vedovato and Gadsby, 2010; Holm et al., 2017).

The lack of passive inward current through G99R made us search for its presence in other situations in which the previous oocyte experiments may not represent the physiological situation in the adrenal cortex (Fig. 9). Inward currents were absent in oocytes expressing G99R at 150 mM  $Na^+_o$ , pH 7.4 (Fig. 9 A), in oocytes

expressing G99R coexpressed with FXD1, which is reportedly expressed in the adrenal gland (Floyd et al., 2010; Fig. 9 B), and at 34°C in 125 mM  $Na^+_o$  (Fig. 9 C). Instead, outward currents were observed in all three cases in the presence of physiological  $K^+_o$ .

To further characterize the loss-of-function induced by G99R, we turned to inside-out patch clamp to compare the  $Na^+_i$  concentration dependence of outward pump currents when  $Na^+_i$  competes with  $K^+_i$  (Fig. 10). Representative current traces from two patches—one excised from an oocyte expressing wild-type (Fig. 10 A) and another from an oocyte expressing G99R pumps (Fig. 10 B), which were held at 0 mV with a pipette solution containing 5 mM  $K^+_o$  in  $NaMG^+_o$ —illustrate that the outward current induced by 4 mM MgATP increases with  $Na^+_i$  concentration. The ATP-induced currents as a function of  $[Na^+_i]$  (Fig. 10 C, symbols) were fitted with a Hill equation (Fig. 10 C, line plots) with parameters  $K_{0.5} = 13.4 \pm 1.2$  mM,  $n_H = 2.9 \pm 0.1$  ( $n = 5$ ) for wild type and  $K_{0.5} = 32.5 \pm 3.7$  mM  $n_H = 1.2 \pm 0.2$  for G99R ( $n = 4$ ). Thus, there is an approximately threefold reduction of apparent  $Na^+_i$  affinity and, perhaps, a loss in apparent cooperativity for  $Na^+_i$  binding at 0 mV. Experiments without  $K^+_i$  (Fig. S3) yielded mean  $K_{0.5} = 2.34 \pm 0.15$ ,  $n_H = 1.2 \pm 0.1$  ( $n = 4$ ) for wild type and  $K_{0.5} = 6.66 \pm 0.54$  mM,  $n_H = 1.2 \pm 0.2$  ( $n = 4$ ) for G99R.

#### $Na^+$ and $K^+$ transport by hyperaldosteronism mutants

Our TEVC measurements in  $Na^+$ -loaded oocytes expressing L104R, V332G, delF100-L104, and EETA963S show that  $K^+_o$  reduces the amplitude of leak currents (Figs. 4 C, 5, and 6), which is consistent with a previous proposal that  $K^+_o$  acts as a nonpermeant, competitive inhibitor of leak currents in the leaky mutants (Azizan

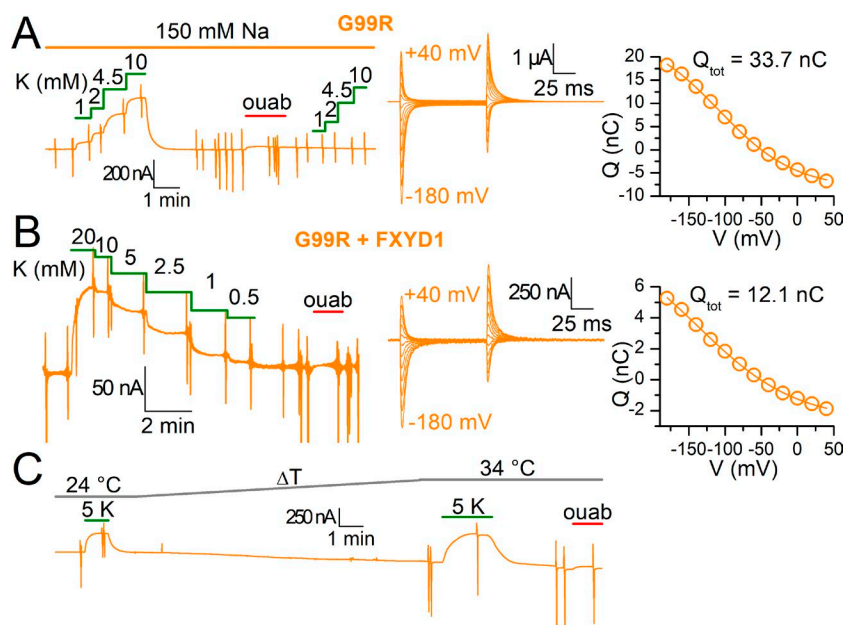


**Figure 9. Function of G99R in 150 mM Na<sup>+</sup><sub>o</sub>, with FXDY1 and at 34°C.** (A) Continuous recording at -50 mV from an oocyte injected with G99R in which increasing K<sup>+</sup><sub>o</sub> concentrations are applied in the presence of 150 mM Na<sup>+</sup><sub>o</sub> (K<sub>0.5</sub>-V plotted in Fig. 8). The ouabain-sensitive currents in Na<sup>+</sup><sub>o</sub> elicited by voltage pulses from -180 to 40 mV, in 20-mV increments, are shown in high temporal resolution in the center. The Q-V curve from those transient currents are shown on the right and was fitted with a Boltzmann distribution (line plot) with parameters Q<sub>tot</sub> = 33.4 nC, V<sub>1/2</sub> = -108 mV, and k = 53 mV. All eight oocytes gave comparable results with inward currents absent from recordings. (B) Current at -50 mV from an oocyte injected with α1-G99Rβ1FXDY1 to which increasing K<sup>+</sup><sub>o</sub> concentrations were applied in the 125 mM Na<sup>+</sup><sub>o</sub>. The transient currents elicited are shown in the center and the Q-V curve from those transient currents are on the right. The Boltzmann distribution (fitted line plot) had parameters Q<sub>tot</sub> = 12.1 nC, V<sub>1/2</sub> = -136 mV, and k = 77 mV. Note that despite robust expression demon-

strated by a large Q<sub>tot</sub>, the total pump current is largely reduced compared with G99R without FXDY1, even at 20 mM K<sup>+</sup><sub>o</sub>. Three oocytes gave similar results with lower pump currents than non-FXYD1 coinjected oocytes. (C) Recording at -50 mV from an oocyte injected with G99R in which application of 5 mM K<sup>+</sup><sub>o</sub> in 125 mM Na<sup>+</sup><sub>o</sub> was performed at 24°C and then at 34°C. Note absence of significant inward current upon application of ouabain, despite deterioration of the oocyte. Three oocytes gave nearly identical results.

et al., 2013), similar to its effect in normal Na/K pumps (Yaragatupalli et al., 2009; Ratheal et al., 2010; Mitchell et al., 2014) where it can also be transported. To test whether the leaky mutants also take up K<sup>+</sup> as part of a somehow distorted Na<sup>+</sup>/K<sup>+</sup> exchange, we measured ouabain-sensitive <sup>86</sup>Rb<sup>+</sup> uptake in oocytes expressing each mutant; Rb<sup>+</sup> is a K<sup>+</sup> congener with nearly identical affinity for the Na/K pump (Forbush, 1987a,b). After a 5-min incubation in Na<sup>+</sup><sub>o</sub> solution with 4.5 mM Rb<sup>+</sup><sub>o</sub> (containing <sup>86</sup>Rb<sup>+</sup>), oocytes that were Na<sup>+</sup> loaded showed significantly larger ouabain-sensitive <sup>86</sup>Rb<sup>+</sup> uptake when injected with any human pump (wild-type,

L104R, V332G, delF100-L104, EETA963S, and G99R pumps) compared with uninjected oocytes (Fig. 11 A). When a 15-min incubation was performed in the same solution, but without preloading the oocytes with Na<sup>+</sup> (to represent more physiological intracellular conditions), oocytes expressing wild type, L104R, V332G, delF100-L104, and EETA963S had significantly more <sup>86</sup>Rb<sup>+</sup> uptake than uninjected oocytes, whereas G99R-injected oocytes had a similarly small uptake (Fig. 11 B). These results demonstrate that (1) the changes in apparent ion affinity in G99R induce a major loss-of-function under physiological conditions, (2) expression of

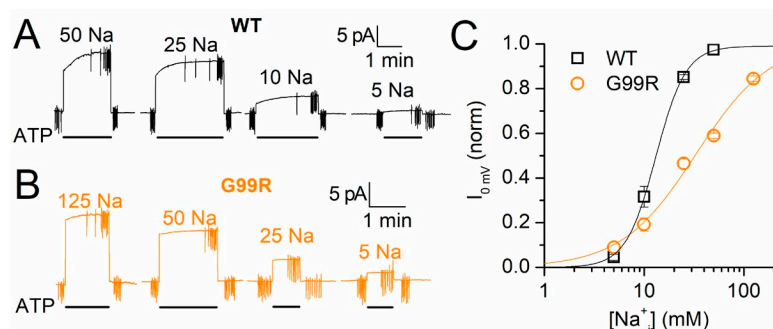


**Figure 10. Na<sup>+</sup><sub>i</sub> dependence of wild-type and G99R pumps.** (A and B) Representative current recordings at 0 mV from giant inside-out patches excised from an oocyte expressing wild type (A) or one expressing G99R (B). The patches were perfused with intracellular solutions of varying [Na<sup>+</sup>]<sub>i</sub> (a mix of Na<sup>+</sup><sub>i</sub> and K<sup>+</sup><sub>i</sub> solutions; Materials and methods). Application of 4 mM ATP induced outward pump currents in a [Na<sup>+</sup>]<sub>i</sub>-dependent manner. Vertical deflections represent 25-ms voltage steps. (C) Mean [Na<sup>+</sup>]<sub>i</sub>-dependence of ATP-induced currents normalized to the I<sub>max</sub> from Hill fits to the mean data for wild type (squares, n = 5) and G99R (circles, n = 4) with parameters K<sub>0.5</sub> = 13.1 mM, n<sub>H</sub> = 2.9 for wild type and K<sub>0.5</sub> = 33.1 mM, n<sub>H</sub> = 1.2 for G99R (mean from fits in individual experiments are shown in the text). Mean ATP-induced current was 12.4 ± 2.6 pA in 50 mM Na<sup>+</sup><sub>i</sub> 90 mM K<sup>+</sup><sub>i</sub> for wild type and 12.4 ± 1.3 pA in 125 mM Na<sup>+</sup><sub>i</sub> for G99R.

G99R does not increase  $\text{Na}^+$  concentration because of a gain-of-function (if it did, it would show increased  $\text{Rb}^+$  uptake without  $\text{Na}^+$  loading), and (3) all leaky mutants increase intracellular  $\text{Na}^+$  concentration to levels large enough for the contribution of L104R, delF100-L104, V332G, and EETA963S to  $^{86}\text{Rb}^+$  uptake to become apparent in the absence of  $\text{Na}^+$  loading.

$\text{Na}^+$  leak through L104R, V332G, delF100-L104, and EETA963S was predicted from the reversal potential measurements (Fig. 6 F) and subsequently confirmed by a 2-h incubation in  $\text{Na}^+$  solution containing  $^{22}\text{Na}^+$  (Fig. 11 C). Also, in agreement with our turnover rate measurements, the observed ouabain-sensitive  $^{22}\text{Na}^+$  influx was larger for mutants with larger turnover rates. Uninjected oocytes and oocytes expressing wild-type or G99R pumps lacked both ouabain-sensitive inward currents and ouabain-sensitive  $\text{Na}^+$  uptake.

## DISCUSSION

In this study we methodically investigated the functional effect of primary aldosteronism mutations to evaluate the structural determinants of previously reported leak currents through these mutants, and we tested the attractive hypothesis (Azizan et al., 2013; Azizan and Brown, 2016) that these leak currents represent a common gain-of-function mechanism producing the pathology associated with all primary aldosteronism-inducing mutations in the Na/K pump. Our results demonstrate that this mechanism cannot explain the effect of at least two of the five mutants studied here because G99R lacks significant inward currents under all conditions and EETA963S produces very small inward currents under physiological extracellular conditions. We discuss our findings in the context of the literature, focusing on the pathway for passive ion permeability in leaky Na/K pump mutants, the nature of the charge carriers for each mutant's inward current, and the deleterious effects of G99R. We conclude with an evaluation of the gain-of-function and loss-of-function hypotheses.

### Structural nature and ion selectivity of the leak pathways

Four out of five Na/K pump mutants studied here (L104R, V332G, EETA963S, and delF100-L104) show steady-state currents representing a noncanonical mode of transport when  $\text{Na}^+$  is the sole external monovalent cation in the solution. Kopec et al. (2014) proposed that the  $\text{Na}^+$  or  $\text{H}^+$  ions carrying the inward leak current through the L104R, V332G, and delF100-L104 mutants traverse a pathway through site II, which differs from the pathway navigated by  $\text{H}^+$  leaking through wild-type (Li et al., 2006) or C-terminally truncated pumps (Yaragatupalli et al., 2009; Meier et al., 2010; Vedovato and Gadsby, 2010), where  $\text{H}^+$  ions are thought to traverse site III (Mitchell et al., 2014; Vedovato and Gadsby,

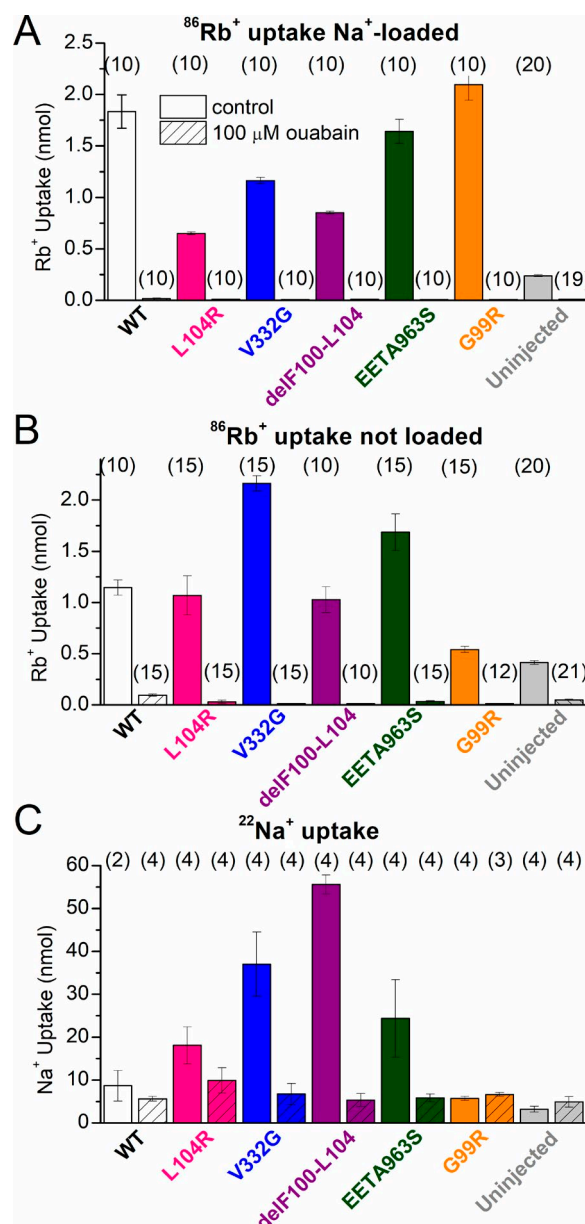


**Figure 11. Radioactive  $^{86}\text{Rb}^+$  and  $^{22}\text{Na}^+$  uptake in oocytes expressing human Na/K pumps.** (A) Mean  $^{86}\text{Rb}^+$  uptake in  $\text{Na}^+$ -loaded oocytes, 4 d after injection, during 5-min incubation in 125 mM  $\text{Na}^+$  with 4.5 mM  $\text{Rb}^+$ , either in the absence (open bars) or presence (striped bars) of 100  $\mu\text{M}$  ouabain. (B) Mean  $^{86}\text{Rb}^+$  uptake in oocytes, 4 d after injection, which were not  $\text{Na}^+$  loaded, during 15-min incubations in the same ionic conditions as in A. In both A and B,  $^{86}\text{Rb}^+$  uptake was also measured in uninjected oocytes from the same batches. (C) Mean  $^{22}\text{Na}^+$  uptake during a 2-h incubation in 125 mM  $\text{Na}^+$  by oocytes expressing wild-type or mutant pumps, 4–5 d after injection in the absence (open bars) or presence (striped bars) of 100  $\mu\text{M}$  ouabain. The number of oocytes is indicated in parentheses above each column. Error bars represent SEM.

2014). We observed that L104R/D933N, V332G/D933N, and delF100-L104/D933N all had inward currents comparable to the parent hyperaldosteronism-associated mutant (Fig. 3), but EETA963S/D933N presented dra-



matically attenuated currents (Figs. 3 and 4). Knowing that D933N obliterates the wild-type  $H^+$  leak (Vedovato and Gadsby, 2014), our findings are consistent with two distinct leaky pathways for hyperaldosteronism-associated Na/K pump mutants: one close to site II (L104R, V332G, and delF100-L104) and another crossing site III (EETA963S), as proposed by Kopec et al. (2014).

At least two lines of evidence demonstrate that all four leaky mutants passively import  $Na^+$ . First, in the absence of  $K^+$ , replacement of  $Na^+$  by  $NMG^+$  shifted the reversal potential of the ouabain-sensitive current by approximately  $-40$  mV in L104R, V332G, and EETA963S, and by approximately  $-100$  mV in delF100-L104. Second, oocytes expressing all four mutants showed increased ouabain-sensitive  $^{22}Na^+$  uptake compared with wild type. These results are in agreement with previous experiments showing mixed permeability to  $Na^+$  and  $H^+$  in L104R (Azizan et al., 2013) and proposals of a higher  $Na^+$  selectivity by delF100-L104 (Azizan et al., 2013; Kopec et al., 2014).

$K^+$  (or  $Rb^+$ ) uptake in pumps engaging in normal  $Na^+/K^+$  exchange transport requires the pump to be phosphorylated. Because phosphorylation requires the presence of intracellular  $Na^+$ , a third, less direct line of evidence indicating  $Na^+$  permeation in V332G and EETA963S is their significantly increased  $^{86}Rb^+$  uptake, even in the absence of  $Na^+$  loading, which contrasts the lack of increased  $^{86}Rb^+$  uptake in G99R-injected oocytes under the same conditions. Whether the  $Rb^+$  transported by L104R and delF100-L104 represents active  $Na^+/K^+$  exchange or occurs via a passive transport mode is unclear; their normal electrogenic transport is clearly impaired, as demonstrated by the tiny or absent outward pump currents induced when  $K^+$  was applied in  $NMG^+$  to oocytes expressing either L104R (comparable to those in uninjected oocytes) or delF100-L104 (which present a small inward current), respectively. Given that these two mutants show outward current (which could simply be a reduction of the inward current, instead of electrogenic  $Na^+/K^+$  transport), it is possible that  $K^+$  (or  $Rb^+$ ) acts as a slowly transported ion, giving the appearance of block.

In any case, because a malfunctioning pump that allows passive  $Na^+$  influx without active  $Na^+$  extrusion would exacerbate the normal workload of wild-type pumps (i.e., half of the pumps in the membrane) encoded by the normal allele, the question with potential pathophysiological relevance is whether each Na/K pump mutant leaks  $Na^+$ . Our data demonstrate that all four leaky mutants passively import  $Na^+$  to different degrees.

#### Turnover rates in leaky mutants: Pump channels or disrupted ion transport?

Of the five primary-aldosteronism-inducing mutations studied here, four (L104R, delF100-L104, V332G, and

EETA963S) showed steady-state leak currents, similar to those previously reported (Azizan et al., 2013), and one (G99R) did not. Whether the inward currents observed in these leaky mutants may represent a "gain-of-function" is quantitatively analyzed below. Turnover rate measurements demonstrate that most hyperaldosteronism-associated leaky mutants transport charge in the order of tens of ions per second, except for delF100-L104 that imports hundreds of ions per second (Fig. 7 and Table 2). These slow turnover values contrast with the much faster transport rates in ion channels ( $10^7$ – $10^8$  s $^{-1}$ ). Thus, none of these Na/K pump  $\alpha 1$  mutants can be considered bona fide channels, like those induced by binding of the Na/K pump-specific marine toxin palytoxin, which opens a pump channel that transports millions of cations per second (Artigas and Gadsby, 2004; Rakowski et al., 2007). Rather, these mutations appear to destabilize ion-occlusion reactions, an effect resembling the alterations produced by deletion or mutation of the  $\alpha$ -subunit C-terminal end, which also induce leaky pumps under near-physiological  $Na^+$  (Yaragatupalli et al., 2009; Meier et al., 2010; Vedovato and Gadsby, 2010). The functional impairment by most hyperaldosteronism-associated mutants is, however, stronger than C-terminal mutants; this is indicated by the smaller-than-wild-type outward currents stimulated by  $K^+$  in L104R, V332G, and delF100-L104, as previously shown by Azizan et al. (2013), in contrast to the wild-type similar currents observed in C-terminal-deleted pumps (Yaragatupalli et al., 2009; Meier et al., 2010; Vedovato and Gadsby, 2010).

#### Functional effects of G99R

On the basis of previous proposals for the mechanism of action of G99R, we expected to observe an inward current (the depolarizing gain-of-function) similar to other TM1 or TM4 mutations (Williams et al., 2014; Gomez-Sanchez et al., 2015; Stindl et al., 2015; Azizan and Brown, 2016). However, our exhaustive examination under a wide range of conditions demonstrates that inward currents are absent in this mutant, even at mammalian physiological  $Na^+$  (150 mM; Fig. 9 A), in the presence of FXD1 (Fig. 9 B), a Na/K pump regulator expressed in the adrenal gland (Floyd et al., 2010), or at near-physiological temperature (34°C; Fig. 9 C). Perhaps more surprising is the observation of outward currents in the presence of physiological  $Na^+$  and  $K^+$ . The maximal current measured in dose-response curves for  $K^+$  in oocytes injected with the human G99R mutant was  $I_{max} = 460 \pm 101$  nA ( $n = 3$ ) at 125 mM  $Na^+$  and  $378 \pm 20$  nA ( $n = 8$ ) at 150 mM  $Na^+$ , way above the  $\sim 25$  nA observed in uninjected oocytes (Fig. 4 A) or oocytes injected with only human  $\beta 1$  cRNA (Stanley et al., 2015). A previous study did not detect ATPase activity in membrane preparations from COS-1 cells expressing rat  $\alpha 1$ -G99R $\beta 1$  pumps (Williams et al., 2014). We have

no explanation for the difference between our oocyte results and the lack of Na/K pump activity in unsided membrane preparations observed by Williams et al. (2014). Nonetheless, these authors found that the rat  $\alpha 1$ -G99R pumps were phosphorylated in the presence of  $\text{Na}^+$  and dephosphorylated by the presence of  $\text{K}^+$  with reduced apparent affinity for the ions, which is fully consistent with our findings. For instance, the dose-response curves for  $\text{K}^+$  show that G99R reduces apparent  $\text{K}^+$  affinity by approximately fourfold at physiological  $\text{Na}^+$  (Fig. 8 C), although this reduction is larger in the absence of  $\text{Na}^+$ , particularly at depolarized voltages, showing an eightfold change in apparent affinity (Fig. S3), nearly identical to the value reported in unsided preparations (Williams et al., 2014).

Given the reduced apparent  $\text{Na}^+$  affinity in G99R, it is surprising that the apparent affinity for  $\text{K}^+$  also decreases in the absence of  $\text{Na}^+$  as the two ions compete for extracellular binding. Reduced Na/K pump affinity for  $\text{Na}^+$  is evident by the displacement of the center of the Q-V curve to more negative voltages (approximately  $-80$  mV), indicating an approximately eightfold reduction in  $\text{Na}^+$  affinity (Fig. 8 D; doubling per each 25-mV shift; Holmgren and Rakowski, 2006). We also evaluated the effect of G99R on the apparent affinity for  $\text{Na}^+$ -dependent pumping in inside-out patches. At 0 mV, G99R reduced apparent  $\text{Na}^+$  affinity approximately threefold in the presence of the physiological competitor  $\text{K}^+$ . Again, this reduction is comparable to measurements of apparent affinity for  $\text{Na}^+$  in membrane preparations (Williams et al., 2014).

Reductions in apparent ion affinity have profound effects on Na/K pump function at physiological concentrations. Under normokalemic conditions ( $\sim 3.5$ – $5$  mM  $\text{K}^+$ ), wild-type pumps are  $\sim 90\%$  saturated with  $\text{K}^+$ , whereas  $\text{K}^+$  binding to G99R pumps would be  $\sim 50\%$  maximal. In addition, the severe hypokalemia regularly seen in hyperaldosteronism patients with somatic Na/K pump mutations (Beuschlein et al., 2013; Williams et al., 2014) will obviously exacerbate this loss-of-function, making pump cycling for G99R even less probable. More convincing evidence for a physiologically relevant loss-of-function in G99R is the similar  $^{86}\text{Rb}^+$  uptake between non- $\text{Na}^+$ -loaded oocytes expressing the G99R mutant and uninjected oocytes, which contrasts the larger  $^{86}\text{Rb}^+$  uptake by oocytes expressing wild-type pumps under the same condition (Fig. 11 B). This reduced  $^{86}\text{Rb}^+$  transport by G99R reflects a decreased apparent affinity for  $\text{Na}^+$ , as robust  $^{86}\text{Rb}^+$  uptake was observed when oocytes were loaded with  $\text{Na}^+$  (Fig. 11 A).

#### Na/K pump loss-of-function as a cause of primary aldosteronism

Absence of inward leak currents through G99R demonstrates that passive inward current is not a necessary gain-of-function for a mutation to induce primary al-

dosteronism. Thus, we propose that the consequences of the G99R mutation point to a clear loss-of-function that underlies primary aldosteronism induction caused by haploinsufficiency. Recently, Nishimoto et al. (2017) identified the premature termination mutant W105stop among several other Na/K pump  $\alpha 1$  mutations in clusters of aldosterone-producing cells that likely represent the transition to aldosterone-producing adenomas. It is very unlikely that W105stop, which ends translation before completing half of the first transmembrane segment, leads to any membrane protein capable of producing a leak current; thus, once again, haploinsufficiency likely accounts for the pathophysiological effects. These results raise an obvious question: is a simple loss-of-function of half the pumps sufficient to increase aldosterone production?

Haploinsufficiency is equivalent to experimentally inhibiting half the pumps. Three studies have shown that ouabain application at concentrations near the  $\text{IC}_{50}$  for Na/K  $\alpha 1$ -pump inhibition (between 10 and 100 nM in bovine cells; Tamura et al., 1996; and at 100  $\mu\text{M}$  ouabain in rat cells; Hajnóczky et al., 1992; Yingst et al., 1999) greatly increases aldosterone production in cultured zona glomerulosa cells. Although this effect was proposed to be mediated by depolarization, on the basis of kinetics (Yingst et al., 1999), the clear difference between the fast kinetics of increasing  $\text{K}^+$  concentration and the slower effects of ouabain (see Fig. 3 in Yingst et al., 1999) indicate that the effect on steroid synthesis is probably secondary to the increase in  $\text{Na}^+$  concentration. The higher  $[\text{Na}^+]$  reduces the driving force for  $\text{Ca}^{2+}$  extrusion through the Na/Ca exchanger. In any case, these results demonstrate that haploinsufficiency (i.e., loss-of-function in half the Na/K pumps) is enough to significantly increase aldosterone production, without the need for an inward current.

Aldosterone production is regulated by membrane voltage. Zona glomerulosa cells present spontaneous voltage oscillations, with amplitude and frequency tightly controlled by the  $\text{K}^+$  gradient (Hu et al., 2012). Membrane depolarization triggers  $\text{Ca}^{2+}$  entry through L-type  $\text{Ca}^{2+}$  channels in rat (Yingst et al., 1999, 2001) and T-type  $\text{Ca}^{2+}$  channels in mice (Hu et al., 2012);  $\text{Ca}^{2+}$  is the second messenger that triggers aldosterone synthesis (Spät, 2004; Hu et al., 2012; Barrett et al., 2016), which translates in increased aldosterone diffusion through the cell membrane. Voltage oscillations in mouse adrenal slices increase their rate by 30% when a rise in external  $\text{K}^+$  from 3 mM to 5 mM depolarized the membrane by 10 mV (Hu et al., 2012). Although spontaneous oscillations under normokalemic conditions are absent in rat isolated cells, an increase in  $\text{K}^+$  from 4 to 7 mM depolarized the resting potential, also by 10 mV, and increased aldosterone production (Lotshaw, 2001).

Two studies report the effect of saturating ouabain on adrenocortical transmembrane voltage. Matthews and

Saffran (1973) showed that application of a saturating concentration of 10  $\mu\text{M}$  ouabain to rabbit adrenocortical cells did not depolarize the membrane for the first 20 min, but an  $\sim 10\text{-mV}$  depolarization followed and persisted through 1 h of perfusion, probably secondary to changes in ionic gradients caused by long-lasting complete Na/K pump inhibition. A similar “sluggish” effect of 10  $\mu\text{M}$  ouabain on membrane potential was reported by Natke and Kabela (1979) in cat adrenocortical cells. Thus, as in most cells, the normal outward Na/K pump current is not a determinant of the adrenocortical membrane potential. Therefore, the effect of haploinsufficiency must be mediated by the reduced  $\text{Na}^+$  gradient because the hypokalemia associated with hyperaldosteronism will help maintain a relatively hyperpolarized voltage.

It follows that for a current to significantly affect transmembrane voltage, its amplitude must be larger than the wild-type Na/K pump current. We measured maximal turnover rates in wild-type pumping and mutant leaks. External  $\text{K}^+$  reduces the amplitude of the inward currents through mutant pumps (Figs. 4 C and 5), although the inward current through the deletion mutant delF100-L104 is clearly much larger than the wild-type pump current at all negative voltages. It is also clear that the presence of nonsaturating  $\text{K}^+$  and  $\text{Na}^+$  will influence the amplitude of the pump current under physiological conditions. The ratio between currents observed in different conditions (e.g., Figs. 4 and 5) allows one to correct the maximal turnover rates to obtain transport rate values at physiological  $\text{Na}^+$  and  $\text{K}^+$ . Hence, wild-type pump current at  $-50\text{ mV}$  in the presence of 125 mM  $\text{Na}^+$  is 0.9 of that observed in  $\text{NMG}^+$  with 3 mM  $\text{K}^+$ . A correction for the effect of normal intracellular  $\text{Na}^+$  is more difficult because  $\text{Na}^+$  widely oscillates from  $\sim 10\text{ mM}$  in cultured cells at rest (van der Bent et al., 1993; Yingst et al., 2001) to  $\sim 50\text{ mM}$  in cells stimulated by angiotensin II (van der Bent et al., 1993). Assuming pumps function at half-maximal capacity, like in many other cells, this results in a turnover rate of  $16\text{ s}^{-1}$ .

The resting potentials reported in adrenal cells are  $-65\text{ mV}$  (in isolated cells from normal adjacent tissues to aldosterone-producing adenomas; Beuschlein et al., 2013) or approximately  $-80\text{ mV}$  (in bovine, rat, and mouse zona glomerulosa cells; Lotshaw, 2001; Hu et al., 2012). Similar corrections can be applied to estimate the relevant inward leak turnover at  $-80\text{ mV}$  through each mutant with 125 mM  $\text{Na}^+$  and 4.5 mM  $\text{K}^+$ . Multiplying the maximal mean turnover rate at  $-50\text{ mV}$  (Table 2) by the ratio between the ouabain-sensitive current in 4.5 mM  $\text{K}^+$  at  $-80\text{ mV}$  (from the I-Vs in Fig. 6) and the  $\text{Na}^+$ -induced current at  $-50\text{ mV}$  (like the one used for turnover measurements, from traces like those in Figs. 4 C and 5) yields turnovers at  $-80\text{ mV}$  of  $t/o_{\text{in}} = 40\text{ s}^{-1}$  for L104R,  $t/o_{\text{in}} = 100\text{ s}^{-1}$  for V332G, and  $t/o_{\text{in}} = 12\text{ s}^{-1}$

for EETA963S. Thus, at  $-80\text{ mV}$ , the ratio between mutant leak current turnover and half-maximal wild-type pump-current turnover is 3.2 for L104R, 6.8 for V332G, 0.8 for EETA963S, and  $521\text{ s}^{-1}$  for delF100-L104.

For the sake of argument, the numbers above were chosen to represent an overestimate of the leak current contributions, based on the assumptions of only half maximal pumping under normal intra and extracellular conditions and a larger hyperpolarized voltage of  $-80\text{ mV}$  in human cells ( $-80\text{ mV}$ , instead of  $-65\text{ mV}$ ). Thus, EETA963S or even L104R are unlikely to induce a pathophysiologically relevant depolarization, but it is conceivable that V332G and delF100-L104 could induce depolarizations like those reported in cells isolated from aldosterone producing adenomas ( $\sim 20\text{ mV}$ ; Beuschlein et al., 2013).

#### Gain-of-function mutant

It is logical to ask, how can we explain the reported depolarizations? Beuschlein et al. (2013) showed an  $\sim 20\text{ mV}$  depolarization in the  $V_m$  of primary cultured adrenal cells from two patients with hyperaldosteronism mutations; this depolarization was  $\text{Na}^+$  dependent and not observed in the healthy tissue from the same patients. However, the actual ATP1A1 mutation present in these patients was not disclosed. Given the amplitude of the depolarization and the strong  $\text{Na}^+$  selectivity, we speculate that at least one (if not both) of those patients carried the delF100-L104 mutation, which has a large enough  $\text{Na}^+$ -selective leak to constitute the proposed gain-of-function. This suspicion is further supported by experiments in the same article, in which the ouabain-resistant rat  $\alpha 1$ -L104R was overexpressed in HEK cells, inducing a smaller depolarization ( $\sim 10\text{ mV}$ ) that was only partially sensitive to  $\text{Na}^+$  removal (Fig. 3 F in Beuschlein et al., 2013). However, reported results from voltage changes in HEK or NCI-H295R cells heterologously expressing ouabain-resistant rat- $\alpha 1$  versions of these mutants (Beuschlein et al., 2013; Williams et al., 2014; Stindl et al., 2015) may overestimate the amplitude of depolarization caused by overexpression; more specifically, overexpressed wild-type pumps may induce a larger-than-normal hyperpolarization in the control group, whereas overexpressed mutants, if leaking, may induce a larger depolarization than they would if expressed at normal levels, resulting in an amplified difference in membrane voltage between wild-type- and mutant-expressing cell groups.

#### Loss-of-function, gain-of-function, or a mixture of both?

All primary hyperaldosteronism mutants present important reductions of their pumping activity under physiological conditions because of the greatly impaired ion-binding affinities (Beuschlein et al., 2013; Williams et al., 2014; Figs. 4, 5, 6, 7, 8, and 9). The lack of inward current or  $\text{Na}^+$  uptake in G99R strongly suggests that



loss-of-function is sufficient to raise the intracellular  $\text{Na}^+$  concentration in cells from aldosterone-producing adenomas carrying these mutations. Toustrup-Jensen et al. (2014) showed that the intracellular  $\text{Na}^+$  concentration is increased in COS-1 cells heterologously expressing Na/K pump mutants with reduced apparent affinity for  $\text{Na}^+$ , providing support to this proposal. Large voltage changes secondary to the changes in ion concentrations are unlikely because the hypokalemia induced by hyperaldosteronism would still hyperpolarize the membrane, even if the  $\text{K}^+$  concentration was somewhat decreased concomitant to the  $\text{Na}^+$  elevation. Thus, we propose that rather than changes in the cell's resting membrane potential, the induction of hyperaldosteronism by G99R, EETA963S, and L104R are caused by the increase in  $\text{Na}^+$  produced by haploinsufficiency, which leads to a reduction of  $\text{Ca}^{2+}$  extrusion or possibly even an increase of  $\text{Ca}^{2+}$  uptake through the Na/Ca exchanger in the reverse mode during each spontaneous depolarization. The Na/Ca exchanger is an important  $\text{Ca}^{2+}$  transport mechanism in zona glomerulosa cells (Kojima and Ogata, 1989; Yingst et al., 2001).

On the basis of the aforementioned arguments, instead of the inward current (i.e., charge inflow) proposed to constitute a gain-of-function leading to depolarization in zona glomerulosa cells carrying leaky Na/K pump mutants (L104R, EETA963S, V332G, or even delF100-L104), it may be the significant passive  $\text{Na}^+$  transport under more physiological intracellular conditions (demonstrated by the increased  $\text{Rb}^+$  uptake in non-loaded oocytes injected with EETA963S and V332G; Fig. 10 B), which leads to the deleterious effects by increasing the  $\text{Na}^+$  load on the wild-type Na/K pump population of the cells. Despite the functional differences between the five Na/K pump mutants documented here, it must be pointed out that all patients, regardless of mutation, present similar symptoms (Azizan et al., 2013; Beuschlein et al., 2013; Dutta et al., 2014; Fernandes-Rosa et al., 2014; Williams et al., 2014, 2016; Åkerström et al., 2015; Wu et al., 2015).

## Conclusion

We have presented a detailed electrophysiological evaluation of five naturally occurring Na/K pump  $\alpha 1$  subunit mutants, which have been linked to primary aldosteronism. In particular, we present the first evaluation of G99R and the first measurement of the turnover rates of transport in each of the previously described mutants known to induce passive inward currents. Based on the compelling data showing an absence of inward current in G99R and the low rate of inward current transport by L104R and EETA963S, we propose an alternative loss-of-function as the minimum common mechanism by which these mutations induce hyperaldosteronism. This haploinsufficiency may or may not be accompanied by the previously proposed gain-of-function.

Measurements of the Na/K pumps' hyperpolarizing outward current, in regard to its contribution to the resting voltage of human zona glomerulosa cells, as well as measurements of the electrophysiological characteristics of cells from aldosterone-producing adenomas harboring known Na/K pump  $\alpha 1$  mutations, will help to definitively solve the mechanisms by which all Na/K pump  $\alpha 1$  mutations induce hyperaldosteronism.

## ACKNOWLEDGMENTS

We thank Dr. Luis Reuss for critically reading the manuscript and Katherine Medina for the RD- $\alpha 1\beta 3$  trace in Fig. 2 A.

This work was supported by the National Science Foundation (grant MCB-1515434 to P. Artigas) and the National Institutes of Health (grant R15-GM061583 to C. Gatto). D.J. Meyer is supported by the American Heart Association (predoctoral fellowship 17PRE32860001).

The authors declare no competing financial interests.

Author contributions: D.J. Meyer performed experiments and analyzed data. D.J. Meyer, C. Gatto, and P. Artigas designed research and wrote the manuscript.

Merritt Maduke served as editor.

Submitted: 20 June 2017

Revised: 25 August 2017

Accepted: 5 September 2017

## REFERENCES

- Åkerström, T., H.S. Willenberg, K. Cupisti, J. Ip, S. Backman, A. Moser, R. Maharjan, B. Robinson, K.A. Iwen, H. Dralle, et al. 2015. Novel somatic mutations and distinct molecular signature in aldosterone-producing adenomas. *Endocr. Relat. Cancer*. 22:735–744. <https://doi.org/10.1530/ERC-15-0321>
- Artigas, P., and D.C. Gadsby. 2004. Large diameter of palytoxin-induced Na/K pump channels and modulation of palytoxin interaction by Na/K pump ligands. *J. Gen. Physiol.* 123:357–376. <https://doi.org/10.1085/jgp.200308964>
- Azizan, E.A., and M.J. Brown. 2016. Novel genetic determinants of adrenal aldosterone regulation. *Curr. Opin. Endocrinol. Diabetes. Obes.* 23:209–217. <https://doi.org/10.1097/MED.0000000000000255>
- Azizan, E.A., H. Poulsen, P. Tuluc, J. Zhou, M.V. Clausen, A. Lieb, C. Maniero, S. Garg, E.G. Bochukova, W. Zhao, et al. 2013. Somatic mutations in ATP1A1 and CACNA1D underlie a common subtype of adrenal hypertension. *Nat. Genet.* 45:1055–1060. <https://doi.org/10.1038/ng.2716>
- Barrett, P.Q., N.A. Guagliardo, P.M. Klein, C. Hu, D.T. Breault, and M.P. Beenhakker. 2016. Role of voltage-gated calcium channels in the regulation of aldosterone production from zona glomerulosa cells of the adrenal cortex. *J. Physiol.* 594:5851–5860. <https://doi.org/10.1111/JP271896>
- Beuschlein, F.S., A. Boulkroun, T. Osswald, H.N. Wieland, U.D. Nielsen, D. Lichtenauer, V.R. Penton, L. Schack, E. Amar, A. Fischer, et al. 2013. Somatic mutations in ATP1A1 and ATP2B3 lead to aldosterone-producing adenomas and secondary hypertension. *Nat. Genet.* 45:440–444. <https://doi.org/10.1038/ng.2550>
- Blanco, G., and R.W. Mercer. 1998. Isozymes of the Na-K-ATPase: heterogeneity in structure, diversity in function. *Am. J. Physiol.* 275:F633–F650.
- Canessa, C.M., J.D. Horisberger, D. Louvard, and B.C. Rossier. 1992. Mutation of a cysteine in the first transmembrane segment of

- Na,K-ATPase alpha subunit confers ouabain resistance. *EMBO J.* 11:1681–1687.
- Choi, M., U.I. Scholl, P. Yue, P. Björklund, B. Zhao, C. Nelson-Williams, W. Ji, Y. Cho, A. Patel, C.J. Men, et al. 2011. K<sup>+</sup> channel mutations in adrenal aldosterone-producing adenomas and hereditary hypertension. *Science*. 331:768–772. <https://doi.org/10.1126/science.1198785>
- Crambert, G., U. Hasler, A.T. Beggah, C. Yu, N.N. Modyanov, J.D. Horisberger, L. Lelièvre, and K. Geering. 2000. Transport and pharmacological properties of nine different human Na<sub>1</sub>K-ATPase isozymes. *J. Biol. Chem.* 275:1976–1986. <https://doi.org/10.1074/jbc.275.3.1976>
- Dutta, R.K., J. Welander, M. Brauckhoff, M. Walz, P. Alesina, T. Arnesen, P. Söderkvist, and O. Gimm. 2014. Complementary somatic mutations of KCNJ5, ATP1A1, and ATP2B3 in sporadic aldosterone producing adrenal adenomas. *Endocr. Relat. Cancer*. 21:L1–L4. <https://doi.org/10.1530/ERC-13-0466>
- Fernandes-Rosa, F.L., T.A. Williams, A. Riester, O. Steichen, F. Beuschlein, S. Boulkroun, T.M. Strom, S. Monticone, L. Amar, T. Meatchi, et al. 2014. Genetic spectrum and clinical correlates of somatic mutations in aldosterone-producing adenoma. *Hypertension*. 64:354–361. <https://doi.org/10.1161/HYPERTENSIONAHA.114.03419>
- Floyd, R.V., S. Wray, P. Martín-Vasallo, and A. Mobasheri. 2010. Differential cellular expression of FXD1 (phospholemman) and FXD2 (gamma subunit of Na<sub>1</sub>K-ATPase) in normal human tissues: a study using high density human tissue microarrays. *Ann. Anat.* 192:7–16. <https://doi.org/10.1016/j.aanat.2009.09.003>
- Forbush, B. III. 1987a. Rapid release of 42K and 86Rb from an occluded state of the Na<sub>1</sub>K-pump in the presence of ATP or ADP. *J. Biol. Chem.* 262:11104–11115.
- Forbush, B. III. 1987b. Rapid release of 42K or 86Rb from two distinct transport sites on the Na<sub>1</sub>K-pump in the presence of Pi or vanadate. *J. Biol. Chem.* 262:11116–11127.
- Galva, C., C. Gatto, and M. Milanick. 2012. Soymilk: an effective and inexpensive blocking agent for immunoblotting. *Anal. Biochem.* 426:22–23. <https://doi.org/10.1016/j.ab.2012.03.028>
- Gatto, C., S.M. McLoud, and J.H. Kaplan. 2001. Heterologous expression of Na<sup>(+)</sup>-K<sup>(+)</sup>-ATPase in insect cells: intracellular distribution of pump subunits. *Am. J. Physiol. Cell Physiol.* 281:C982–C992.
- Geering, K. 2008. Functional roles of Na<sub>1</sub>K-ATPase subunits. *Curr. Opin. Nephrol. Hypertens.* 17:526–532. <https://doi.org/10.1097/MNH.0b013e3283036cbf>
- Gomez-Sanchez, C.E., M. Kuppasamy, and E.P. Gomez-Sanchez. 2015. Somatic mutations of the ATP1A1 gene and aldosterone-producing adenomas. *Mol. Cell. Endocrinol.* 408:213–219. <https://doi.org/10.1016/j.mce.2014.12.004>
- Hajnoczky, G., G. Csordás, L. Hunyady, M.P. Kalapos, T. Balla, P. Enyedi, and A. Spät. 1992. Angiotensin-II inhibits Na<sup>(+)</sup>/K<sup>(+)</sup> pump in rat adrenal glomerulosa cells: possible contribution to stimulation of aldosterone production. *Endocrinology*. 130:1637–1644.
- Hannemann, A., M. Bidlingmaier, N. Friedrich, J. Manolopoulou, A. Spyroglou, H. Völzke, F. Beuschlein, J. Seissler, R. Rettig, S.B. Felix, et al. 2012. Screening for primary aldosteronism in hypertensive subjects: results from two German epidemiological studies. *Eur. J. Endocrinol.* 167:7–15. <https://doi.org/10.1530/EJF-11-1013>
- Holm, R., J. Khandelwal, A.P. Einholm, J.P. Andersen, P. Artigas, and B. Vilsen. 2017. Arginine substitution of a cysteine in transmembrane helix M8 converts Na<sub>1</sub>K-ATPase to an electroneutral pump similar to H<sup>(+)</sup>/K<sup>(+)</sup>-ATPase. *Proc. Natl. Acad. Sci. USA*. 114:316–321. <https://doi.org/10.1073/pnas.1617951114>
- Holmgren, M., and R.F. Rakowski. 2006. Charge translocation by the Na<sup>(+)</sup>/K<sup>(+)</sup> pump under Na<sup>(+)</sup>/Na<sup>(+)</sup> exchange conditions: intracellular Na<sup>(+)</sup> dependence. *Biophys. J.* 90:1607–1616. <https://doi.org/10.1529/biophysj.105.072942>
- Holmgren, M., J. Wagg, F. Bezanilla, R.F. Rakowski, P. De Weer, and D.C. Gadsby. 2000. Three distinct and sequential steps in the release of sodium ions by the Na<sup>(+)</sup>/K<sup>(+)</sup>-ATPase. *Nature*. 403:898–901. <https://doi.org/10.1038/35002599>
- Hu, C., C.G. Rusin, Z. Tan, N.A. Guagliardo, and P.Q. Barrett. 2012. Zona glomerulosa cells of the mouse adrenal cortex are intrinsic electrical oscillators. *J. Clin. Invest.* 122:2046–2053. <https://doi.org/10.1172/JCI61996>
- Kanai, R., H. Ogawa, B. Vilsen, F. Cornelius, and C. Toyoshima. 2013. Crystal structure of a Na<sup>(+)</sup>-bound Na<sub>1</sub>K-ATPase preceding the E1P state. *Nature*. 502:201–206. <https://doi.org/10.1038/nature12578>
- Kaplan, J.H. 2002. Biochemistry of Na<sub>1</sub>K-ATPase. *Annu. Rev. Biochem.* 71:511–535. <https://doi.org/10.1146/annurev.biochem.71.102201.141218>
- Koenderink, J.B., S. Geibel, E. Grabsch, J.J. De Pont, E. Bamberg, and T. Friedrich. 2003. Electrophysiological analysis of the mutated Na<sub>1</sub>K-ATPase cation binding pocket. *J. Biol. Chem.* 278:51213–51222. <https://doi.org/10.1074/jbc.M306384200>
- Kojima, I., and E. Ogata. 1989. Na-Ca exchanger as a calcium influx pathway in adrenal glomerulosa cells. *Biochem. Biophys. Res. Commun.* 158:1005–1012. [https://doi.org/10.1016/0006-291X\(89\)92822-2](https://doi.org/10.1016/0006-291X(89)92822-2)
- Kopeck, W., B. Loubet, H. Poulsen, and H. Khandelia. 2014. Molecular mechanism of Na<sup>(+)</sup>/K<sup>(+)</sup>-ATPase malfunction in mutations characteristic of adrenal hypertension. *Biochemistry*. 53:746–754. <https://doi.org/10.1021/bi401425g>
- Laemmli, U.K. 1970. Cleavage of structural proteins during the assembly of the head of bacteriophage T4. *Nature*. 227:680–685. <https://doi.org/10.1038/227680a0>
- Li, C., O. Capendeguy, K. Geering, and J.D. Horisberger. 2005. A third Na<sup>(+)</sup>-binding site in the sodium pump. *Proc. Natl. Acad. Sci. USA*. 102:12706–12711. <https://doi.org/10.1073/pnas.0505980102>
- Li, C., K. Geering, and J.D. Horisberger. 2006. The third sodium binding site of Na<sub>1</sub>K-ATPase is functionally linked to acidic pH-activated inward current. *J. Membr. Biol.* 213:1–9. <https://doi.org/10.1007/s00232-006-0035-0>
- Lotshaw, D.P. 2001. Role of membrane depolarization and T-type Ca<sup>2+</sup> channels in angiotensin II and K<sup>(+)</sup> stimulated aldosterone secretion. *Mol. Cell. Endocrinol.* 175:157–171. [https://doi.org/10.1016/S0303-7207\(01\)00384-7](https://doi.org/10.1016/S0303-7207(01)00384-7)
- Matsudaira, P. 1987. Sequence from picomole quantities of proteins electroblotted onto polyvinylidene difluoride membranes. *J. Biol. Chem.* 262:10035–10038.
- Matthews, E.K., and M. Saffran. 1973. Ionic dependence of adrenal steroidogenesis and ACTH-induced changes in the membrane potential of adrenocortical cells. *J. Physiol.* 234:43–64. <https://doi.org/10.1113/jphysiol.1973.sp010333>
- Meier, S., N.N. Tavaraz, K.L. Dürr, and T. Friedrich. 2010. Hyperpolarization-activated inward leakage currents caused by deletion or mutation of carboxy-terminal tyrosines of the Na<sup>(+)</sup>/K<sup>(+)</sup>-ATPase alpha subunit. *J. Gen. Physiol.* 135:115–134. <https://doi.org/10.1085/jgp.200910301>
- Mitchell, T.J., C. Zugarramurdi, J.F. Olivera, C. Gatto, and P. Artigas. 2014. Sodium and proton effects on inward proton transport through Na<sub>1</sub>K pumps. *Biophys. J.* 106:2555–2565. <https://doi.org/10.1016/j.bpj.2014.04.053>
- Mulatero, P., M. Stowasser, K.C. Loh, C.E. Fardella, R.D. Gordon, L. Mosso, C.E. Gomez-Sanchez, F. Veglio, and W.F. Young Jr. 2004. Increased diagnosis of primary aldosteronism, including surgically correctable forms, in centers from five continents. *J.*

- Clin. Endocrinol. Metab.* 89:1045–1050. <https://doi.org/10.1210/jc.2003-031337>
- Natke, E. Jr., and E. Kabela. 1979. Electrical responses in cat adrenal cortex: possible relation to aldosterone secretion. *Am. J. Physiol.* 237:E158–E162.
- Nishimoto, K., M. Koga, T. Seki, K. Oki, E.P. Gomez-Sanchez, C.E. Gomez-Sanchez, M. Naruse, T. Sakaguchi, S. Morita, T. Kosaka, et al. 2017. Immunohistochemistry of aldosterone synthase leads the way to the pathogenesis of primary aldosteronism. *Mol. Cell. Endocrinol.* 441:124–133. <https://doi.org/10.1016/j.mce.2016.10.014>
- Price, E.M., and J.B. Lingrel. 1988. Structure-function relationships in the sodium-potassium-ATPase alpha subunit: site-directed mutagenesis of glutamine-111 to arginine and asparagine-122 to aspartic acid generates a ouabain-resistant enzyme. *Biochemistry.* 27:8400–8408. <https://doi.org/10.1021/bi00422a016>
- Rakowski, R.F., P. Artigas, F. Palma, M. Holmgren, P. De Weer, and D.C. Gadsby. 2007. Sodium flux ratio in Na/K pump-channels opened by palytoxin. *J. Gen. Physiol.* 130:41–54. <https://doi.org/10.1085/jgp.200709770>
- Ratheal, I.M., G.K. Virgin, H. Yu, B. Roux, C. Gatto, and P. Artigas. 2010. Selectivity of externally facing ion-binding sites in the Na/K pump to alkali metals and organic cations. *Proc. Natl. Acad. Sci. USA.* 107:18718–18723. <https://doi.org/10.1073/pnas.1004214107>
- Rossi, G.P., G. Bernini, C. Caliumi, G. Desideri, B. Fabris, C. Ferri, C. Ganzaroli, G. Giacchetti, C. Letizia, M. Maccario, et al. PAPY Study Investigators. 2006. A prospective study of the prevalence of primary aldosteronism in 1,125 hypertensive patients. *J. Am. Coll. Cardiol.* 48:2293–2300. <https://doi.org/10.1016/j.jacc.2006.07.059>
- Sachse, F.B., R. Clark, and W.R. Giles. 2017. No fuzzy space for intracellular Na(+) in healthy ventricular myocytes. *J. Gen. Physiol.* 149:683–687. <https://doi.org/10.1085/jgp.201711826>
- Spät, A. 2004. Glomerulosa cell—a unique sensor of extracellular K<sup>+</sup> concentration. *Mol. Cell. Endocrinol.* 217:23–26. <https://doi.org/10.1016/j.mce.2003.10.046>
- Stanley, C.M., D.G. Gagnon, A. Bernal, D.J. Meyer, J.J. Rosenthal, and P. Artigas. 2015. Importance of the Voltage Dependence of Cardiac Na/K ATPase Isozymes. *Biophys. J.* 109:1852–1862. <https://doi.org/10.1016/j.bpj.2015.09.015>
- Stanley, K.S., D.J. Meyer, C. Gatto, and P. Artigas. 2016. Intracellular Requirements for Passive Proton Transport through the Na(+),K(+)-ATPase. *Biophys. J.* 111:2430–2439. <https://doi.org/10.1016/j.bpj.2016.09.042>
- Stindl, J., P. Tauber, C. Sterner, I. Tegtmeier, R. Warth, and S. Bandulik. 2015. Pathogenesis of Adrenal Aldosterone-Producing Adenomas Carrying Mutations of the Na(+)/K(+)-ATPase. *Endocrinology.* 156:4582–4591. <https://doi.org/10.1210/en.2015-1466>
- Tamura, M., D.W. Piston, M. Tani, M. Naruse, E.J. Landon, and T. Inagami. 1996. Ouabain increases aldosterone release from bovine adrenal glomerulosa cells: role of renin-angiotensin system. *Am. J. Physiol.* 270:E27–E35.
- Tavraz, N.N., T. Friedrich, K.L. Dürr, J.B. Koenderink, E. Bamberg, T. Freilinger, and M. Dichgans. 2008. Diverse functional consequences of mutations in the Na<sup>+</sup>/K<sup>+</sup>-ATPase alpha2-subunit causing familial hemiplegic migraine type 2. *J. Biol. Chem.* 283:31097–31106. <https://doi.org/10.1074/jbc.M802771200>
- Toustrup-Jensen, M.S., A.P. Einholm, V.R. Schack, H.N. Nielsen, R. Holm, M.J. Sobrido, J.P. Andersen, T. Clausen, and B. Vilsen. 2014. Relationship between intracellular Na<sup>+</sup> concentration and reduced Na<sup>+</sup> affinity in Na<sup>+</sup>,K<sup>+</sup>-ATPase mutants causing neurological disease. *J. Biol. Chem.* 289:3186–3197. <https://doi.org/10.1074/jbc.M113.543272>
- van der Bent, V., C. Demole, E.I. Johnson, M.F. Rossier, C.P. Python, M.B. Vallotton, and A.M. Capponi. 1993. Angiotensin-II induces changes in the cytosolic sodium concentration in bovine adrenal glomerulosa cells: involvement in the activation of aldosterone biosynthesis. *Endocrinology.* 133:1213–1220. <https://doi.org/10.1210/endo.133.3.8365363>
- Vedovato, N., and D.C. Gadsby. 2010. The two C-terminal tyrosines stabilize occluded Na/K pump conformations containing Na or K ions. *J. Gen. Physiol.* 136:63–82. <https://doi.org/10.1085/jgp.201010407>
- Vedovato, N., and D.C. Gadsby. 2014. Route, mechanism, and implications of proton import during Na<sup>+</sup>/K<sup>+</sup> exchange by native Na<sup>+</sup>/K<sup>+</sup>-ATPase pumps. *J. Gen. Physiol.* 143:449–464. <https://doi.org/10.1085/jgp.201311148>
- Wang, X., and J.D. Horisberger. 1995. A conformation of Na(+)-K<sup>+</sup> pump is permeable to proton. *Am. J. Physiol.* 268:C590–C595.
- Williams, T.A., S. Monticone, V.R. Schack, J. Stindl, J. Burrello, F. Buffolo, L. Annaratone, I. Castellano, F. Beuschlein, M. Reincke, et al. 2014. Somatic ATP1A1, ATP2B3, and KCNJ5 mutations in aldosterone-producing adenomas. *Hypertension.* 63:188–195. <https://doi.org/10.1161/HYPERTENSIONAHA.113.01733>
- Williams, T.A., M. Peitzsch, A.S. Dietz, T. Dekkers, M. Bidlingmaier, A. Riester, M. Treitl, Y. Rhayem, F. Beuschlein, J.W. Lenders, et al. 2016. Genotype-Specific Steroid Profiles Associated With Aldosterone-Producing Adenomas. *Hypertension.* 67:139–145. <https://doi.org/10.1161/HYPERTENSIONAHA.115.06186>
- Wu, V.C., K.H. Huang, K.Y. Peng, Y.C. Tsai, C.H. Wu, S.M. Wang, S.Y. Yang, L.Y. Lin, C.C. Chang, Y.H. Lin, et al. 2015. Prevalence and clinical correlates of somatic mutation in aldosterone producing adenoma-Taiwanese population. *Sci. Rep.* 5:11396. <https://doi.org/10.1038/srep11396>
- Yaragatupalli, S., J.F. Olivera, C. Gatto, and P. Artigas. 2009. Altered Na<sup>+</sup> transport after an intracellular alpha-subunit deletion reveals strict external sequential release of Na<sup>+</sup> from the Na/K pump. *Proc. Natl. Acad. Sci. USA.* 106:15507–15512. <https://doi.org/10.1073/pnas.0903752106>
- Yingst, D.R., J. Davis, S. Krenz, and R.J. Schiebinger. 1999. Insights into the mechanism by which inhibition of Na,K-ATPase stimulates aldosterone production. *Metabolism.* 48:1167–1171. [https://doi.org/10.1016/S0026-0495\(99\)90133-6](https://doi.org/10.1016/S0026-0495(99)90133-6)
- Yingst, D.R., J. Davis, and R. Schiebinger. 2001. Effects of extracellular calcium and potassium on the sodium pump of rat adrenal glomerulosa cells. *Am. J. Physiol. Cell Physiol.* 280:C119–C125.
- Zheng, F.F., L.M. Zhu, A.F. Nie, X.Y. Li, J.R. Lin, K. Zhang, J. Chen, W.L. Zhou, Z.J. Shen, Y.C. Zhu, et al. 2015. Clinical characteristics of somatic mutations in Chinese patients with aldosterone-producing adenoma. *Hypertension.* 65:622–628. <https://doi.org/10.1161/HYPERTENSIONAHA.114.03346>